IN-13

135314

P.55

NASA
Technical
Memorandum

NASA TM-108385

A PLAN FOR SPACECRAFT AUTOMATED RENDEZVOUS

By A.W. Deaton, J.J. Lomas, and L.D. Mullins

Systems Analysis and Integration Laboratory
Science and Engineering Directorate

October 1992

(NASA-TM-108385) A PLAN FOR
SPACECRAFT AUTOMATED RENDEZVOUS
(NASA)   55 p

N93-15392

Unclas

G3/13   0135314

NASA
National Aeronautics and
Space Administration

George C. Marshall Space Flight Center

MSFC · Form 3190 (Rev. May 1983)

REPORT DOCUMENTATION PAGE

1. AGENCY USE ONLY *(Leave blank)*	2. REPORT DATE October 1992	3. REPORT TYPE AND DATES COVERED Technical Memorandum

4. TITLE AND SUBTITLE

A Plan for Spacecraft Automated Rendezvous

5. FUNDING NUMBERS

6. AUTHOR(S)

A.W. Deaton, J.J. Lomas, and L.D. Mullins

7. PERFORMING ORGANIZATION NAME(S) AND ADDRESS(ES)

George C. Marshall Space Flight Center
Marshall Space Flight Center, Alabama 35812

8. PERFORMING ORGANIZATION REPORT NUMBER

9. SPONSORING/MONITORING AGENCY NAME(S) AND ADDRESS(ES)

National Aeronautics and Space Administration
Washington, DC 20546

10. SPONSORING/MONITORING AGENCY REPORT NUMBER

NASA TM-108385

11. SUPPLEMENTARY NOTES

Prepared by Systems Analysis and Integration Laboratory, Science and Engineering Directorate.

12a. DISTRIBUTION/AVAILABILITY STATEMENT

Unclassified—Unlimited

12b. DISTRIBUTION CODE

13. ABSTRACT *(Maximum 200 words)*

An automated rendezvous approach has been developed that utilizes advances in technology to reduce real-time/near real-time flight operations support personnel to an acceptable level that is near the minimum without jeopardizing the success of the mission. The on-board flight targeting uses a rule-based system to select the pursuit vehicle phasing orbits and uses precise navigation updates from the pursuit/target spacecraft made possible by the global positioning system receivers/processors on both spacecraft to adjust the phasing orbits and achieve rendezvous. The ascent-to-orbit targeting for the pursuit vehicle has been successfully decoupled from the on-orbit orbit transfer phasing targeting. Typical launch window data have been developed for the heavy lift launch vehicle and cargo transfer vehicle for a Space Station *Freedom* rendezvous mission.

14. SUBJECT TERMS Rendezvous, Phasing, Launch Window, Targeting, Insertion Surface			15. NUMBER OF PAGES 55
			16. PRICE CODE NTIS
17. SECURITY CLASSIFICATION OF REPORT Unclassified	18. SECURITY CLASSIFICATION OF THIS PAGE Unclassified	19. SECURITY CLASSIFICATION OF ABSTRACT Unclassified	20. LIMITATION OF ABSTRACT Unlimited

TABLE OF CONTENTS

Page

LIST OF ILLUSTRATIONS

LIST OF ILLUSTRATIONS (Continued)

TECHNICAL MEMORANDUM

A PLAN FOR SPACECRAFT AUTOMATED RENDEZVOUS

I. INTRODUCTION

This report describes a rendezvous targeting approach which takes advantage of the technology developments in computers and navigation instruments to make it possible to achieve automated flight from lift-off to rendezvous with a target spacecraft. The ultimate goal is to greatly reduce the real-time flight operations support personnel normally required to successfully achieve rendezvous of a pursuit vehicle (PV) and a passive S/C. The method by which the ascent to orbit across a given launch window can be decoupled from the on-orbit targeting and how small adjustments can be made near launch to reflect improvements in the knowledge of the target S/C state vector (position and velocity vectors or orbital elements) are described.

The enabling technology that makes automated rendezvous possible is the global positioning system (constellation of 24 navigation satellites) which makes onboard precision navigation possible. If both the PV and target S/C are equipped with global positioning system (GPS) receivers/processors and the target S/C navigation state is transmitted to ground and relayed to the PV, then the targeting can be adjusted by onboard computations to accomplish S/C rendezvous. The GPS can be used in the absolute navigation mode[1] (100 m and 1 m/s accuracy) and in a relative navigation mode[2] (10 m and 0.1 m/s) using the S/C GPS information. The relative navigation mode allows the PV to close to a position near enough to the target to permit the proximity sensors to acquire the target and reach a position to be captured by (grappled) or docked to the target spacecraft. The GPS, when integrated with the inertial navigation system, can be used to derive the absolute navigation state, relative navigation state, and attitude state of the PV. If the PV was equipped with a GPS receiver/processor and the target S/C was not equipped with such a system, a long-range (radar) sensor would be required to derive the relative navigation state. Although PV automated rendezvous would still be possible, the flight profile would require an acquisition phase, a longer timeline, and more propellant (ΔV).

The term "automated flight" or "automated rendezvous" refers to an onboard system that steps through a sequence of events, including orbit transfers, based upon a given flight plan with limited adjustment capability to achieve PV/target S/C rendezvous with little assistance from a ground support team. The ground support team establishes the launch window opening and closing times, the basic ascent to orbit targeting parameters, and the basic flight plan and targeting data for the on-orbit PV, and would intervene only when some failure precludes successful execution of the flight plan. The on-orbit phasing orbits and orbit transfer times can be determined onboard by a rule-based targeting algorithm. What has been discussed is referred to as automated rendezvous. An autonomous rendezvous, requiring no help from the ground except for contingencies, is believed to be too large a step for this point in the technology development.

II. ASCENT VEHICLE LAUNCH WINDOW

A few concepts need to be defined prior to describing the ascent vehicle launch window to support a rendezvous mission. In the case of rendezvous where a target vehicle (TV), such as a space station, is already in orbit and it is desired to launch a second or PV, such as a cargo transfer vehicle[4] (CTV), so that the two vehicles may be brought together (rendezvoused) within a reasonably small time

period (a few hours or a few days) and with a reasonably small amount of fuel expenditure on the part of either vehicle, then the dynamics of the problem requires that the PV be launched into (or nearly into) the same plane as the TV. Since the TV is in a plane which is nearly fixed in inertial space and, while on the launch pad, the PV is rotating rapidly (~15°/h) with respect to the TV plane, there will be only one or two times per day when the PV can be launched into the same plane as the TV. Determining the time (or times) on any given day when this can be accomplished constitutes the determination of the PV launch window. This problem will be described in some detail in this section and addressed further in the next section. Given a TV in an orbit with an orbital inclination (angle between the Equator and orbital plane) greater than the launch site latitude, the launch site will rotate under the TV orbital plane twice per day as illustrated by figure 1.
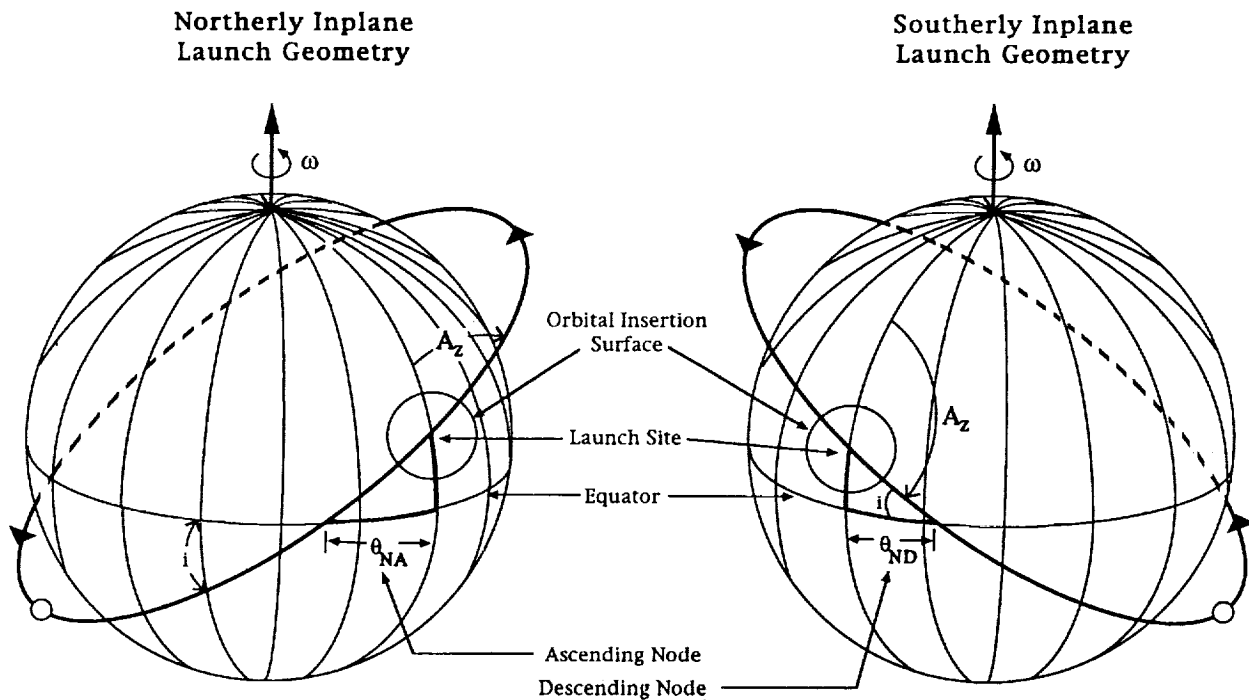
Figure 1. In-plane launch geometry.

Should the TV orbital inclination be equal to the latitude of the launch site, only one in-plane alignment of the launch site occurs each day. The basic flight profile for an in-plane launch, one requiring little or no out-of-plane (yaw) steering, will create a unique inclination for each flight azimuth (angle from north to selected flight plane) utilized. The nodal crossing angle or angle between a reference point on the Equator (Greenwich Meridian, launch site meridian, vernal equinox, etc.) and the resulting orbital flight plane intersection in addition to the orbital inclination fully define the orbital plane at any instant of time. The nodal crossing angles for ascending and descending nodes are illustrated by figure 1.

If the orbital inclination of the PV is fixed at the in-plane value and the nodal crossing angle is varied by the Earth rotational rate (slightly adjusted for differential nodal regression), the plane of a target satellite can be tracked across a launch window (lift-off time variation from an opening to closing time). As the nodal crossing angle is varied from the in-plane value, the launch azimuth should vary to reduce the launch vehicle performance penalty. A typical set of launch window data has been generated for a heavy lift launch vehicle (HLLV) for an orbital inclination compatible with a due-east launch (latitude of launch site equal to the orbital inclination). Figure 2 shows how the performance of the launch vehicle is penalized as the descending node angle (referenced from the launch site meridian space fixed at lift-off) is varied from the in-plane value (near 90°) by the Earth rotational rate times the time

2

from the in-plane lift-off time ($WE^*\Delta T$) and also given as a function of time prior (– values) to the in-plane alignment and past (+ values) that alignment. The penalty for not varying the launch azimuth (set at due-east value or 90°) is also illustrated. If the acceptable launch vehicle performance penalty was set at 1,134 kg (2,500 lb), the launch window available would open at about 47 min prior to the in-plane alignment and close at 34 min past that alignment. The sensitivity of the performance is highly dependent upon the launch vehicle characteristics and the suborbital conditions at closed-loop guidance (path adaptive vehicle steering closed around the navigational state) release. The nonsymmetry of the performance penalty is caused by the early launch ($AZ < 90°$) being in a more favorable velocity condition with respect to the inertial Earth rotational velocity than the late launch.

DESCENDING NODE MEASURED FROM LAUNCH SITE
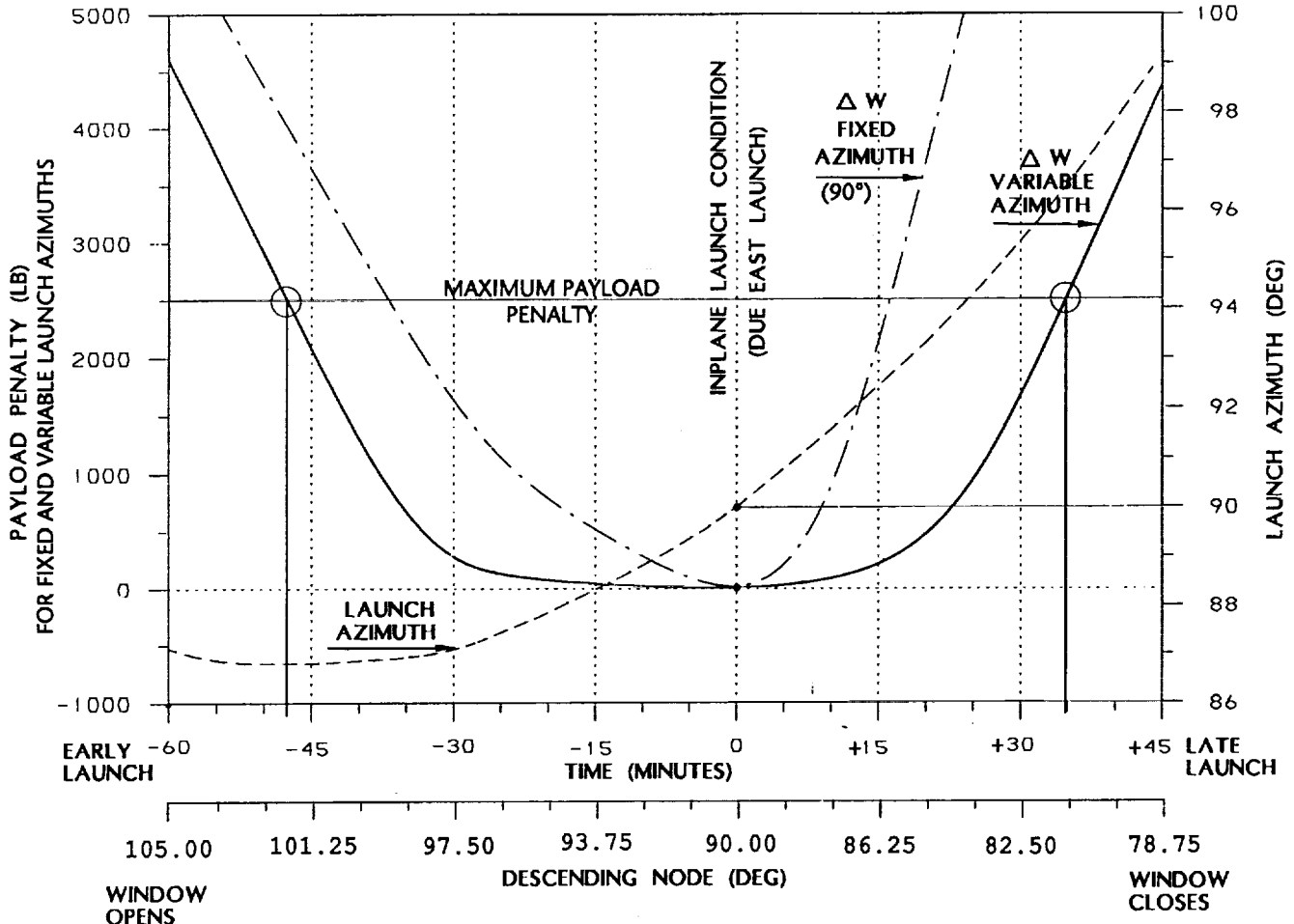
Figure 2. HLLV launch window data.

By defining a standard insertion orbit for the PV (upper stage, CTV, etc.) it is possible to create an orbital insertion surface[3] across the acceptable launch window with the in-plane orbital elements fixed and the nodal crossing angle given as a function of launch azimuth. This technique decouples the ascent vehicle launch window targeting data from the on-orbit targeting. The PV phasing geometry, the differential nodal regression between PV/TV orbits, and other constraints dictate the azimuth versus launch window time function (connecting link between the ascent targeting and on-orbit targeting). The details of this targeting procedure are discussed in section IV.

3

III. TARGET SPACECRAFT PHASE WINDOW

A. Problem Formulation

The TV's state, a six-dimensional state vector (which also defines its orbit plane), will be specified at some arbitrary time prior to the PV's desired launch. This state can then be propagated forward in time by some high quality ephemeris generator such that the state of the TV is known continuously as a function of time. This orbit plane described relative to an inertial system (for example, mean-of-1950; mean-of-date, etc.) will have a fixed inclination relative to the Earth's equatorial plane, and the right ascension of its ascending node (RAN) will slowly regress relative to this inertial system at the rate of about $-7°$/day. (This regression is caused by the oblateness of the Earth, and its exact value is a function of the orbital elements.)

The PV, assumed launched from Kennedy Space Center (KSC), will have a known state vector at main engine cutoff (MECO) whose Earth-fixed coordinates will depend only on the launch azimuth, but whose inertial coordinates will depend on the launch time; i.e., day-of-year and time-of-day. Once the PV is launched, its orbit will be inertially fixed as defined by its MECO vector, and its orbit plane will then behave in the same qualitative manner as the TV's orbit plane; i.e., its inclination will remain fixed and its line-of-nodes will regress in time although at a slightly different rate than that of the TV if its orbit is slightly different in size. Figure 3 shows all of this geometry. The idea of the launch window is to pick the time-of-day to launch so that the orbit plane of the PV is aligned with (or is co-planar with) that of the TV. This occurs approximately when the launch site (KSC) rotates through (or into) the orbit plane of the TV. If the inclination of the TV's plane is greater than the latitude of the launch site (KSC), then there will be two times per day when this occurs as explained in the previous section. If the latitude of the launch site is equal to the inclination of the TV's orbit plane, then this will occur once per day. This is assumed to be the case in this study.

B. Problem Solution

At any given starting time (day and hour), the TV's state vector is provided in terms of inertial, osculating orbital elements, $\bar{X}_{TVO} = (a,e,i,\omega,\Omega,v)_o$. At this time, the angle between the Greenwich Meridian (the Earth-fixed reference) and the vernal equinox (the inertially fixed reference) can be calculated. This angle is called the Greenwich hour angle of the vernal equinox or more simply the Greenwich sidereal time (GST). As illustrated in figure 3, it measures the angular separation between the inertially fixed reference system and the Earth-fixed reference system. This angle increases at the rotational rate of the Earth or at 15.041°/mean solar hour. It goes through 360° in just under 1 day.

The right ascension of the ascending node of the target orbit (Ω) measures the orientation of the target orbit plane relative to the inertial system, and the longitude of the ascending node (λ_{AN}) measures the orientation of the target orbit plane relative to the Earth-fixed system. From figure 3, it is easy to see that these angles are related by

$$\lambda_{AN_{target}} = \Omega - GST , \tag{1}$$

and

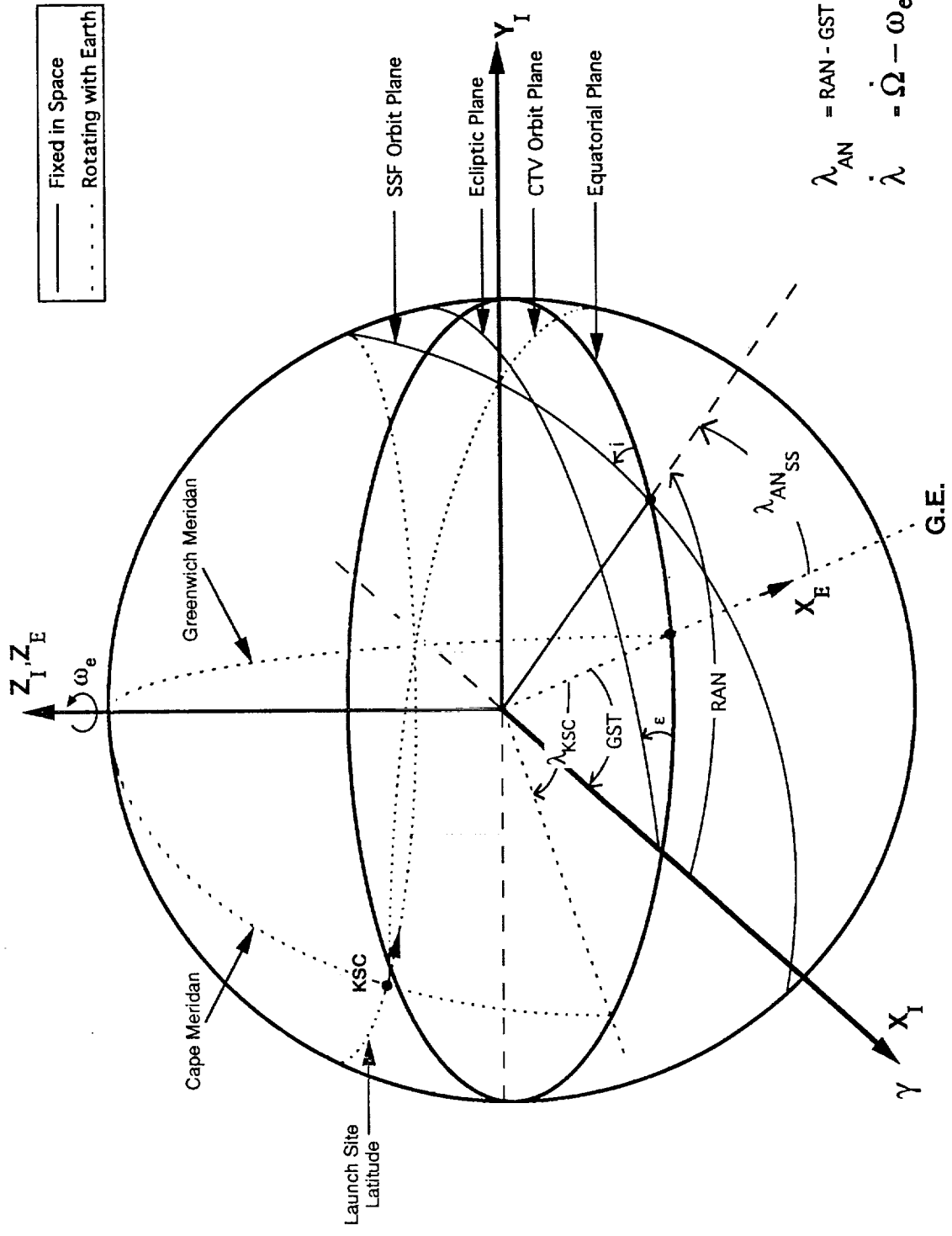$$\dot{\lambda}_{AN_{target}} = \dot{\Omega} - \omega_e . \tag{2}$$

4

Figure 3. Inertially fixed and Earth-fixed (rotating) reference systems.

For a due-east launch of the PV, its MECO vector will be specified by the elements, $\bar{X}_{PV_{MECO}} = (a,e,i,\omega,\lambda_{AN},\nu)_{MECO}$. The fifth element of this set is the longitude of its ascending node. This makes it independent of the launch time.

Since there is a time associated with the TV's state vector, it is possible to calculate the longitude of its ascending node at that time by use of equation (1). The longitude of the TV's orbit node continually changes at the rate given by equation (2). What is desired is to have the longitude of the ascending nodes of the two orbit planes coincide at MECO. To calculate the wait time or time to launch, measured from the time at which the TV's state vector was initially given (a more or less arbitrary reference time), we take the difference in the longitudes of the ascending nodes of the two orbits at that reference time and divide by the rate at which the TV's longitude is changing (equation (2)).

$$\Delta MET = \frac{\lambda_{AN_{o_{target}}} - \lambda_{AN_{pursuit}}}{\omega_e - \dot{\Omega}_{target}}.$$ (3)

This time, added to the initial or reference time of the TV's orbit, is the MECO time for the PV

$$GMT_{pursuit_{MECO}} = GMT_{o_{target}} + \Delta MET .$$ (4)

This GMT at MECO of the PV minus the ascent time of the PV from launch to MECO gives the required launch time (GMT) of the PV to put it in-plane with the target at MECO

$$GMT_{pursuit_{launch}} = GMT_{pursuit_{MECO}} - MET_{pursuit_{MECO}} .$$ (5)

These in-plane launch opportunities occur approximately once per day. The delta time between consecutive in-plane opportunities is

$$\Delta time = \frac{360°}{\omega_e - \dot{\Omega}} ,$$ (6)

which is about $23^{1}/2$ hours, the exact value depending on the orbit of the TV.

The initial state vector and time of the TV and the MECO vector of the PV along with equations (1) through (5) determine the time of the in-plane launch opportunity for the PV. The launch window will be some variation on either side of the in-plane opportunity.

In addition to determining the in-plane launch time, it is also necessary to determine the two state vectors at the in-plane time so that the relative position or phase of the two vehicles may be known at that time. This will be an essential ingredient in determining the rendezvous profile and required rendezvous time.

The target state at the pursuit MECO in-plane time is obtained by propagating the initial target state vector forward in time by the elapsed time calculated in equations (3) and (4). The phase angle, defined as the difference in the arguments-of-latitude (the in-plane position or angle of a satellite relative to its ascending node) of the target and the PVs, can be calculated at that time as

$$\phi_o = \Delta u = u_{target_{MECO}} - u_{pursuit_{MECO}} = (\omega + \nu)_{target} - (\omega + \nu)_{pursuit} .$$ (7)

The magnitude of this phase angle determines the amount of time required for the PV to rendezvous with the TV.

6

C. Variations Across the Launch Window; No Yaw Steering

By varying the launch time by ±45 min on either side of the in-plane launch and holding all parameters on the PV MECO vector constant (due-east, in-plane launches; no yaw steering), it is then possible to determine the difference in the longitudes (and also the right ascensions) of the ascending nodes of the pursuit and target orbit planes across the launch window:

(1) The state vector of the pursuit stays constant across the launch window

(2) The longitude of the ascending node of the target varies at the rate given by equation (2)

(3) The actual target longitude of ascending node at any time from the in-plane time is

$$\lambda_{AN_{target}} = \lambda_{AN_{target_{in-plane}}} + \dot{\lambda}_{AN_{target}} * \Delta LT \ . \tag{8}$$

In addition to the longitude of the ascending node of the target orbit plane varying across the launch window, the phase angle also varies across the launch window (because of the launch time variation, ΔLT) and, hence, the time required for the pursuit to rendezvous with the target. At orbital insertion, with no yaw steering, the u (argument-of-latitude) of the pursuit will always be the same value, but the u of the target is a function of the delta time between the actual launch time and the in-plane launch time. For a near-circular target orbit, the position of the target in its orbit plane across the launch window is

$$u_{target} = u_{0_{target}} + \bar{u}_{target} * \Delta LT \ , \tag{9}$$

where

$$\bar{u}_{target} = \dot{n}_{target} + \bar{\omega}_{target} \ , \tag{10}$$

where $\bar{\omega}$ is the apsidal rotation rate and where $\dot{n}_{target}$ is the perturbed mean motion of the target. $\Delta LT < 0$ for early launches and $\Delta LT > 0$ for late launches

The phase angle across the launch window is

$$\phi = u_{target} - u_{pursuit} \ ,$$

$$\phi = u_{0_{target}} + \bar{u}_{target} * \Delta MET - u_{pursuit} \ . \tag{11}$$

Figure 4 shows the delta longitude of ascending nodes between the target and PV orbit planes for a typical case with no yaw steering of the PV across the launch window. Figure 5 shows the variation in phase angle for the same case across the launch window.

D. Launch Window With Variable Azimuth and Yaw Steering

It would be too expensive, propellant-wise, on-orbit to take out the delta longitude between the pursuit and target orbit planes shown in figure 4. This angle will be removed with the booster during the ascent trajectory by using yaw steering along with a fixed or a variable launch azimuth. Since, as can be seen from figure 2 in section II, the payload loss is much less with a variable launch azimuth, this will be assumed to be the form of the operational ascent trajectory. The ΔMET away from the in-plane launch time (or, equivalently, the delta longitude shown in fig. 4) will determine the variable azimuth and the
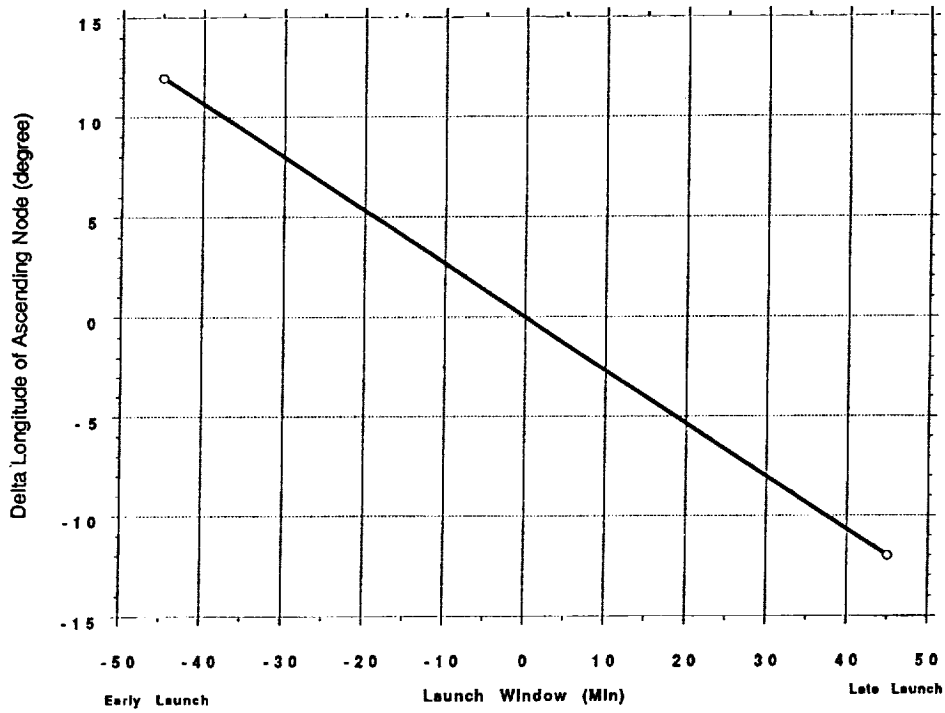
7

Figure 4. Delta longitude of ascending node of TV/PV
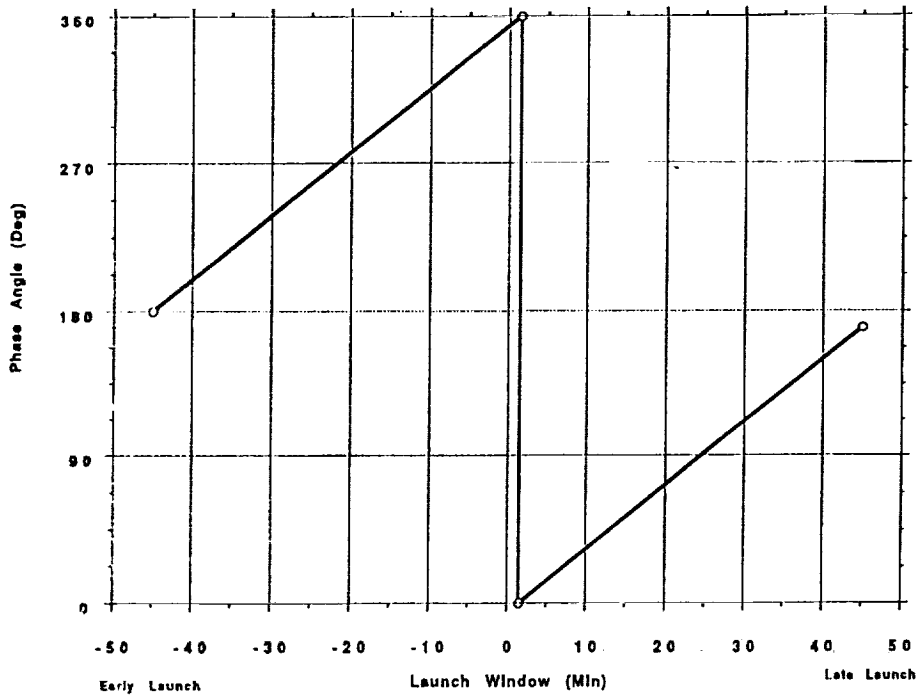across launch window using no yaw steering.

Figure 5. Phase angle between TV and PV at MECO across launch window
using fixed launch azimuth (sample case).

amount of yaw steering required of the ascent trajectory to reach MECO in an in-plane condition (no delta longitude). There will be a corresponding payload penalty accompanying each of these "off-nominal" or "nonoptimum" cases, but that is the price to be paid for a finite or nonzero launch window for the PV. The shape of the ascent trajectory, the cutoff conditions, and the payload penalty will depend to some degree on the guidance algorithm used to fly the ascent trajectory. The ascent trajectory program used here to illustrate the problem is called the Program to Optimize Simulated Trajectories (POST).[5]

The POST program steers the ascent trajectory of the PV such that the cutoff (MECO) values of the semimajor axis (a), eccentricity (e), inclination (i), and the true anomaly (v) for all launch azimuths are the same as the in-plane or 90° launch azimuth case. The longitude of the ascending node at MECO is varied making the delta longitude of ascending node (shown in fig. 4 for the in-plane launches) equal to zero all across the launch window.

The initial phase angle for the in-plane case (with due-east launch azimuth and with no yaw steering), calculated by equation (11) is shown in figure 5. With variable launch azimuth across the launch window, as shown in figure 2 of section II, and with yaw steering, the cutoff argument-of-perigee (ω) of the PV varies across the launch window as shown in figure 6. This variable argument-of-perigee causes the initial phase angle ϕ of the variable-azimuth-with-yaw-steering case to vary from the fixed-azimuth-with-no-yaw-steering case (shown in fig. 5) by the same amount as the initial argument-of-perigee shown in figure 6.

Across the launch window, one can see the longitude of the ascending node in figure 7, the payload loss in figure 2 of section II, and the insertion phase angle, ϕ, in figure 8. If one compares figure 8 to figure 5, it can be seen that at the in-plane time (0 min) the phase angles are the same, and at the extreme ends of the window (±45 min) the phase angles are about 10° different; the same difference as the variation in argument-of-perigee shown in figure 6.

The initial phase angle between the TV and the PV, shown in figure 8, will be used to calculate the required rendezvous time between the TV and the PV as will be explained in detail in the next section. The phase angles shown in figures 5 and 8 should be taken only as typical or representative values. In actual cases, the phase angle will vary according to what the initial state vector and time of the TV may be and with what the MECO conditions of the PV may be. In summary, the methods given here are sufficient to generate the initial phase angle curve (fig. 8) for any and all sets of initial conditions which may be given.

The phase angle (the difference in the angular positions of the TV and the PV in their common orbit plane) is gradually reduced in time by the two vehicles traveling at different angular rates dictated by the difference in (mean) orbital altitudes of the two orbits. The catch-up rate is a function of the difference in the size of the two orbits; the greater the difference in orbit size, the larger the catch-up rate. It is obvious that the larger the initial phase angle is, the larger will be the required rendezvous time, but there are subtleties associated with this that require more detailed explanation which will be provided later. Rendezvous is accomplished by reducing the difference in angular positions (phase angle) to zero while at the same time reducing the difference in the "size" of the orbits to zero and reducing the relative velocities to zero. The technique of doing this is the subject of the next section.
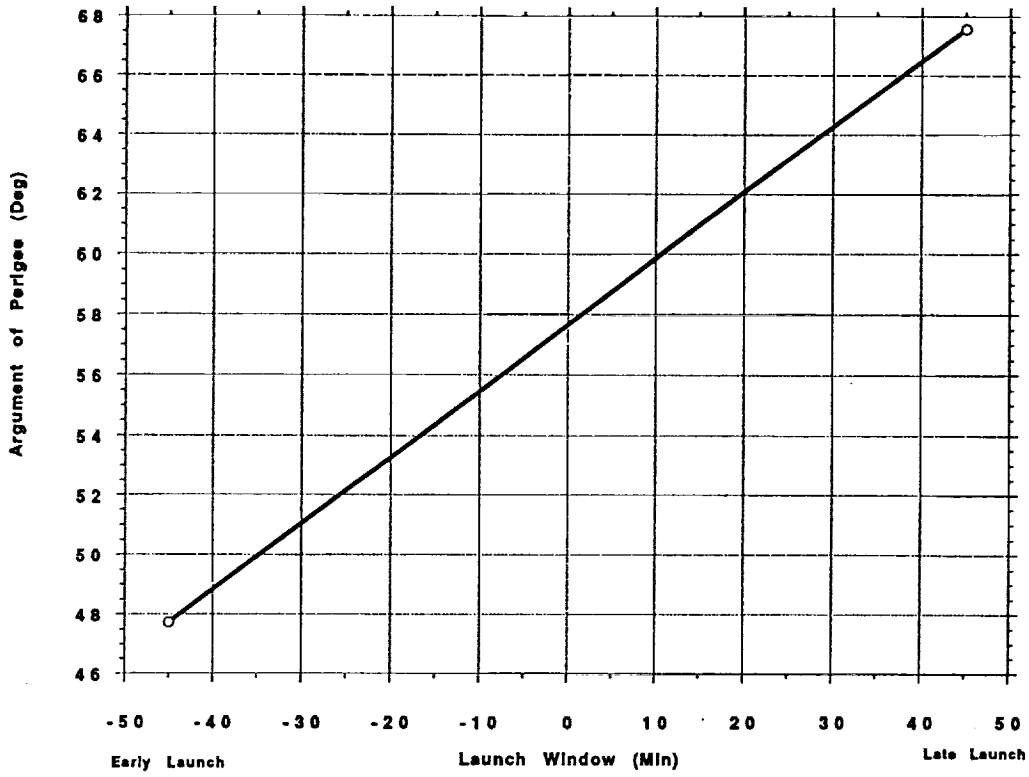
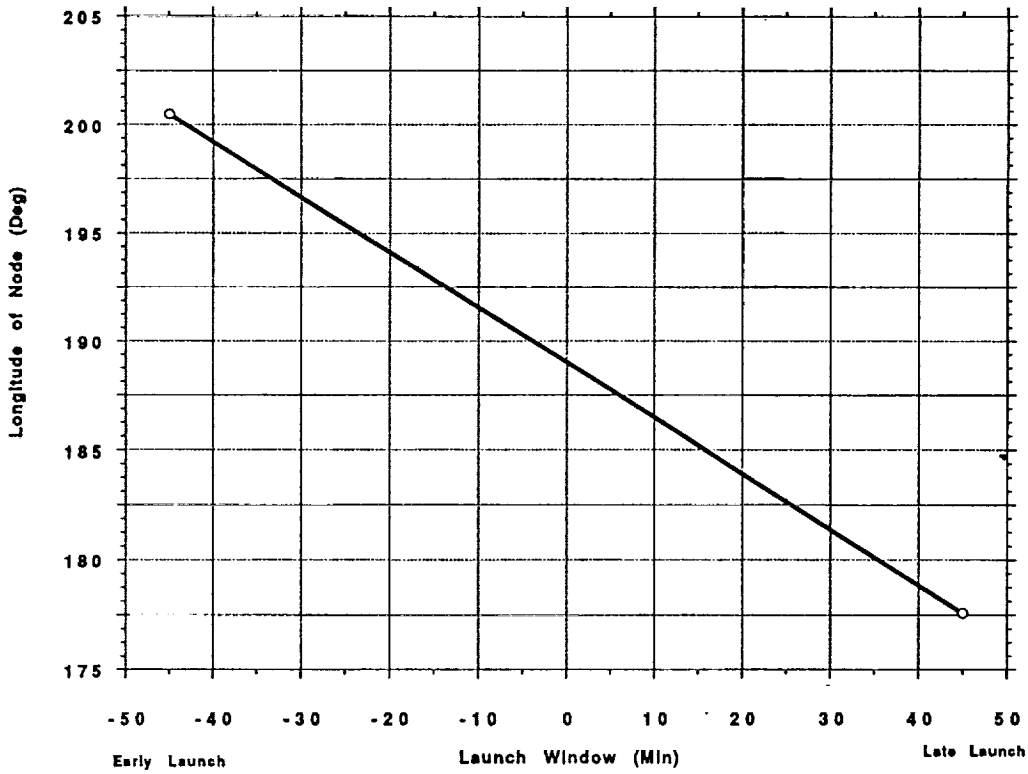Figure 6. Argument of perigee of PV across launch window using variable azimuth launch.

Figure 7. Longitude of ascending node of PV across launch window using variable azimuth launch.

10
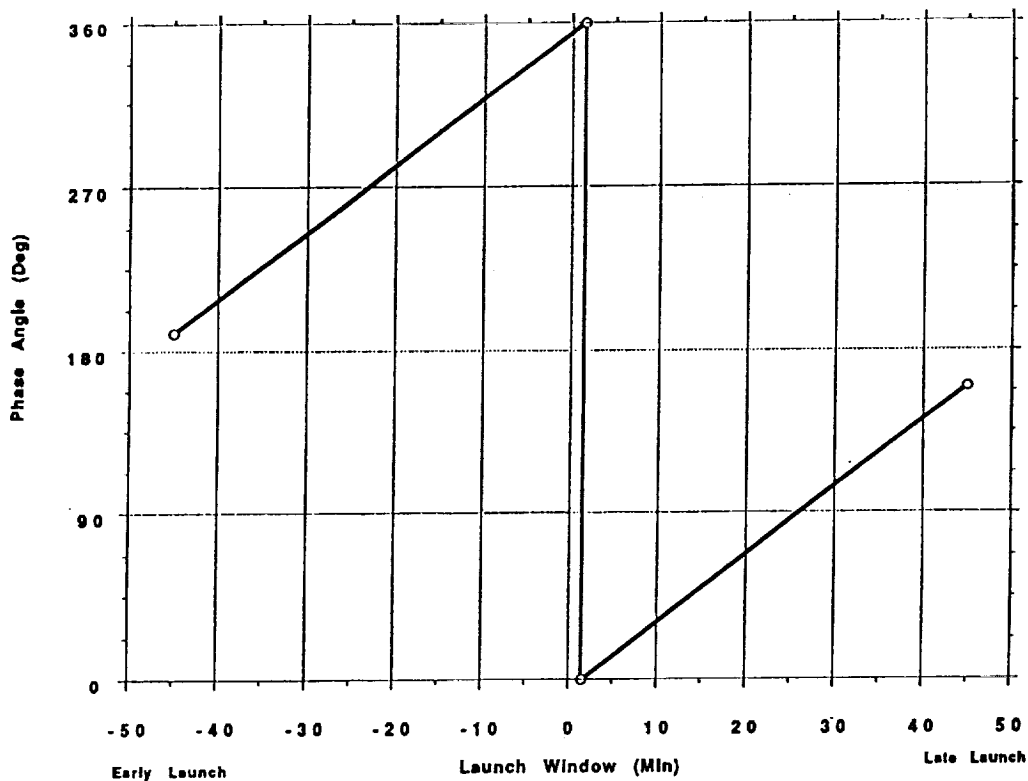
Figure 8. Phase angle between TV and PV at MECO across launch window
using variable azimuth launch.

IV. MISSION PROFILE, PHASING STRATEGY, AND RULE-BASED TARGETING

To achieve a spacecraft automated rendezvous, it is important to standardize the mission profile to the extent possible thereby simplifying the on-board targeting algorithms. The mission profile must have phase (central angle between the PV/TV) adjustment capability to compensate for launch time variation across the launch window, orbit transfer execution errors, navigation errors, orbit propagation errors, and target ephemeris errors. There are a number of mission profiles and phasing strategies, such as double coelliptical rendezvous, that can be automated to achieve the desired rendezvous mission. The mission profile and phasing strategy to be described in this section will use the heavy lift launch vehicle (HLLV) configuration with a cargo transfer vehicle (CTV) to place the cargo at S.S. *Freedom*. The HLLV (proposed vehicle) is to be built from space shuttle propulsion system parts in which two advanced solid rocket motors (ASRM's) or two redesigned solid rocket motors (RSRM's) would be mounted to a stretched space shuttle external tank (ET) with either six space shuttle main engines (SSME's) or six space transportation main engines (STME's) mounted on a boattail below the ET. The inline nature of the design leads to a flight profile very similar to that of the space shuttle where, after the SRM's are spent and jettisoned, the core stage or ET is placed in an orbit with the perigee altitude at approximately 30 km (16 nmi) and apogee altitude at the desired final orbit height (400 km). The ET will reenter the atmosphere and the orbiter, or in this case the CTV, will execute an orbit transfer burn to raise the radius of perigee (low point in orbit) to a safe altitude (150 km) or circularize the orbit. The mission profile as outlined here was baselined for the HLLV first design cycle and is illustrated by figure 9.

11
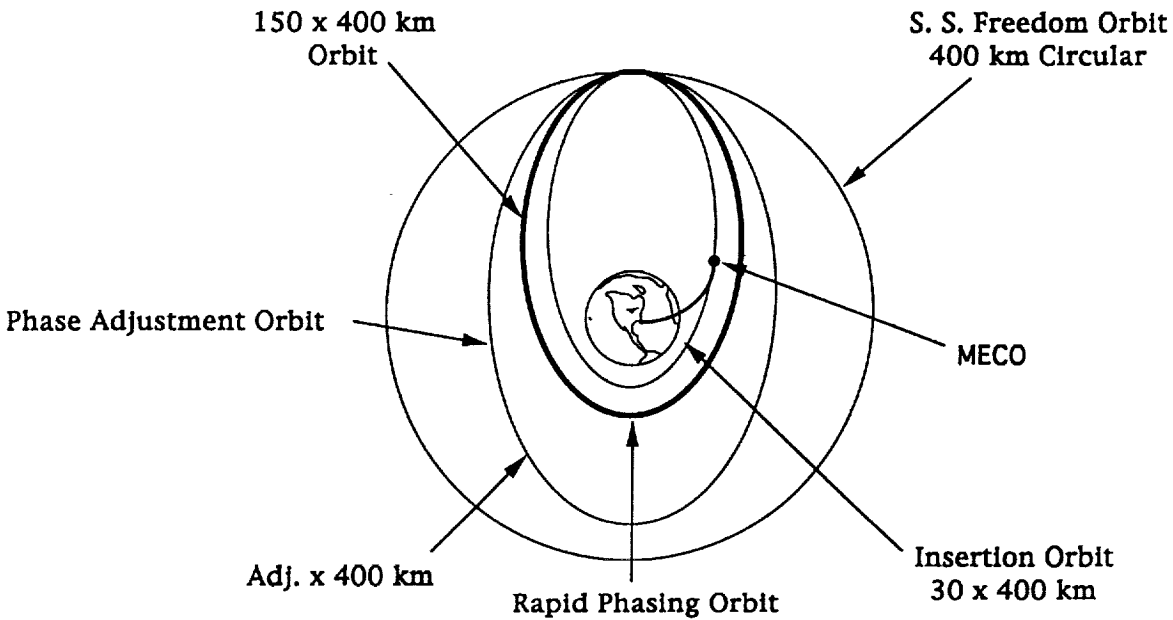
Figure 9. Orbit phase adjustment.

A. Phasing Strategy

In the first HLLV design cycle, the 150×400-km orbit (fig. 9) was used as a rapid phasing orbit with a minimum number of revolutions set at two prior to executing a phase adjustment orbit transfer at apogee. The phase adjustment orbit was set at a perigee altitude of 275 km with a minimum of two and one half revolutions used prior to a rendezvous transfer burn executed at perigee (165° transfer) to enforce a stable orbit (same orbit) rendezvous (SOR) position 37 km (20 nmi) behind S.S. *Freedom*. Figure 10 shows, for the example case, the mission time required from MECO to SOR insertion as a function of initial phase angle relationship (between CTV and S.S. *Freedom*). As the initial phase angle increases, additional revs are required in the rapid phasing orbit. Note the minimum mission time possible is approximately 10 h (dictated by a minimum of 2 revs in the rapid phasing orbit, 2½ revs in phase adjustment orbit and the 165° transfer to SOR).

The linear nature of the phase relationship of S.S. *Freedom* with respect to the in-plane alignment of the launch site on a day-to-day basis was described in section III. The phase relationship of the pursuit/target can be any value between "0°" and "360°" when the launch site in-plane condition occurs. By shifting the opening and closing of the launch window (section II), the phase relationship can be changed. If the 2,500-lb payload loss limit launch window penalty for the HLLV is used in conjunction with the phase/time data from figure 10, the maximum mission time (lift-off to SOR) versus minimum launch window, as given by figure 11, could be derived. Figure 11 gave the worst mission time using the phase shift penalty of 2,500-lb payload loss to guarantee a given launch window duration. To guarantee a minimum launch window of 15 min every day regardless of the in-plane phase relationship, then the

12

Figure 10. Relative phase angle at insertion.

Figure 11. CTV launch window analysis.

13

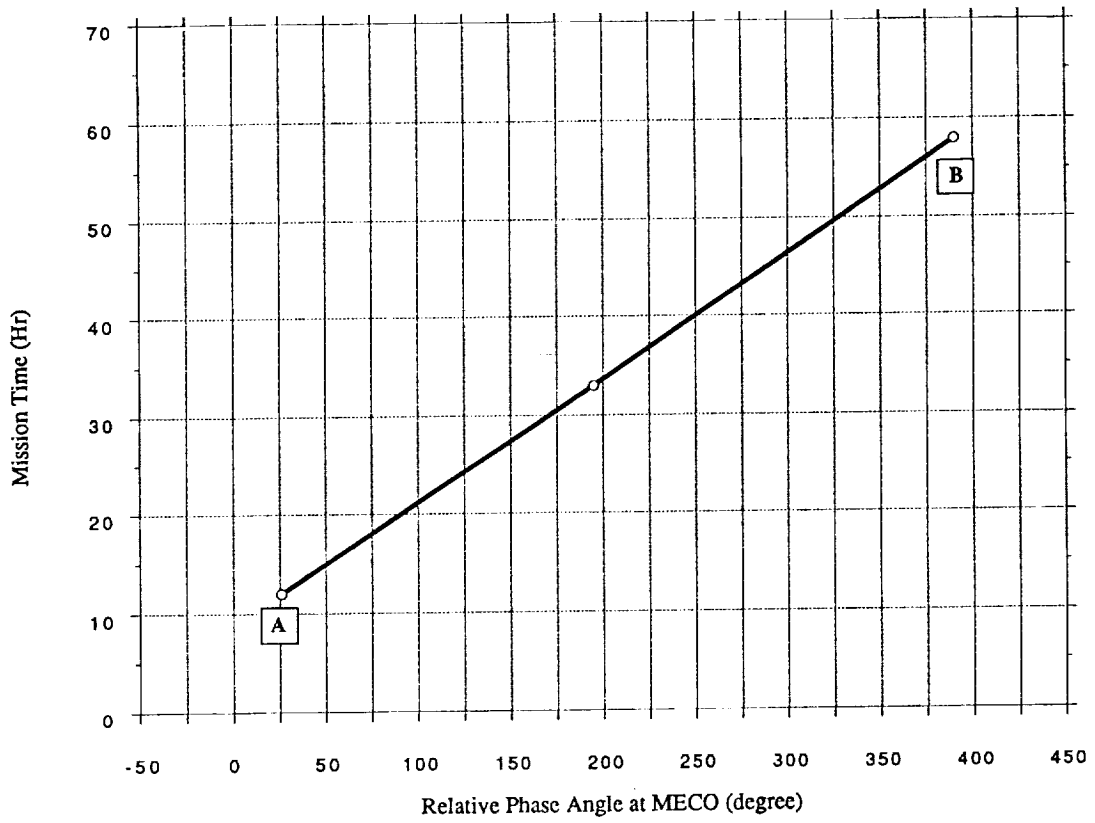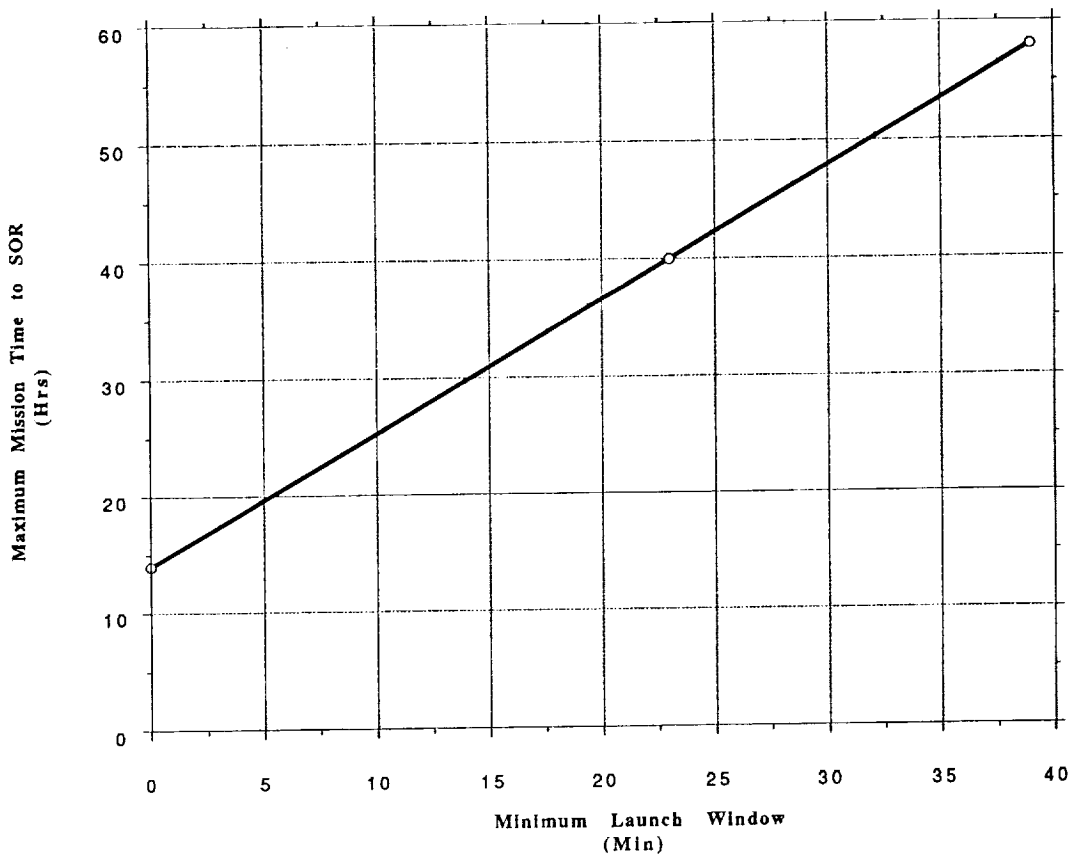maximum mission time was 30 h. There were, of course, days when the mission time was less than 30 h with still a 15-min launch window or with a greater launch window within the 30-h mission time. These data were based on an S.S. *Freedom* circular orbit altitude of 400 km inclined 28.5° to the Equator. This simplified phasing scheme was used to generate these trend data. In actual practice, the apogee height would not be equal to the target orbit nor intersect it, but would be targeted below the target orbit so that the natural growth of apogee caused by the finite burns would not cause an intersection with the target orbit. Intersection with the target orbit would occur during the stable orbit rendezvous maneuver. This particular phasing strategy was designed to allow the PV to always add energy to the orbit. Shorter mission times could be achieved by phasing from a lower circular or near-circular orbit, or in some instances, a higher near-circular orbit, but at the cost of more propellant and less cargo.

Using the HLLV/CTV data from the first design cycle, the CTV targeting process can be described as follows:

1. Determine the time that the launch site rotates into S.S. *Freedom's* orbital plane (in this case, the time a due-east launch orbit insertion with no yaw steering lies in S.S. *Freedom's* orbital plane).

2. Determine the time required for the CTV to drive the phase difference to zero (radius vectors parallel) using no CTV yaw steering and a preselected flight profile strategy.

3. Using the nodal difference between CTV and S.S. *Freedom* at SOR (Δ node) from step 2, determine the lift-off time correction for the HLLV (Δ node/Earth's rotational rate).

4. Since this lift-off time correction will change the CTV/S.S. *Freedom* phase relationship, repeat steps 2 through 3 until the nodal difference and phase difference are within an acceptable tolerance.

The HLLV targeting for orbital insertion remains unchanged; only the time of lift-off for the due-east launch has been adjusted for the CTV no-yaw steering compatibility. Next, an early launch can be adjusted in the same way as the in-plane launch condition by using the orbital insertion generated from a launch azimuth based on a given estimated descending node angle measured from the launch site meridian. This new HLLV orbital insertion surface will have a different phase relationship with S.S. *Freedom* and must be adjusted for the differential node regression the same way as the in-plane due-east launch. These time adjustments (lift-off time adjustment) can be developed for the full launch window, and the HLLV orbital insertion targeting is thereby decoupled from CTV on-orbit targeting. The HLLV would simply be targeted to a given ellipse (30×400 km) and orbital plane (inclination and node) as a function of flight azimuth. The CTV targeting would set the launch window opening and closing times and the azimuth versus time in the launch window. A useful output of this targeting process is the nodal angle bias as a function of phase angle (fig. 12). These data (nodal bias) would be needed onboard the CTV to assure planar alignment at the SOR point.

B. Rule-Based Targeting

To successfully develop an automated rule-based targeting technique for spacecraft rendezvous, one needs a general flight profile or flight plan that is simple and easy to implement considering the guidance and navigation system available. The targeting strategy developed for the CTV will be used as an example of rule-based targeting. To describe the targeting technique, refer to figure 13 in which
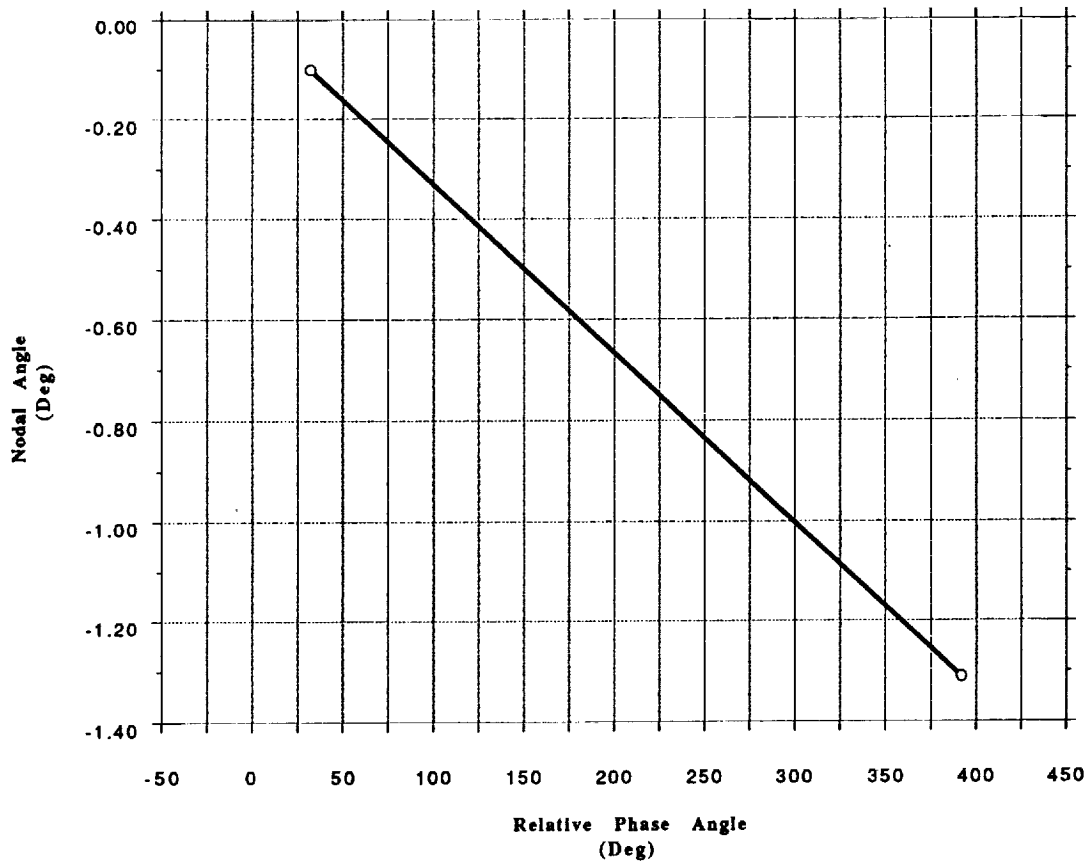
Figure 12. Nodal bias versus phase angle.
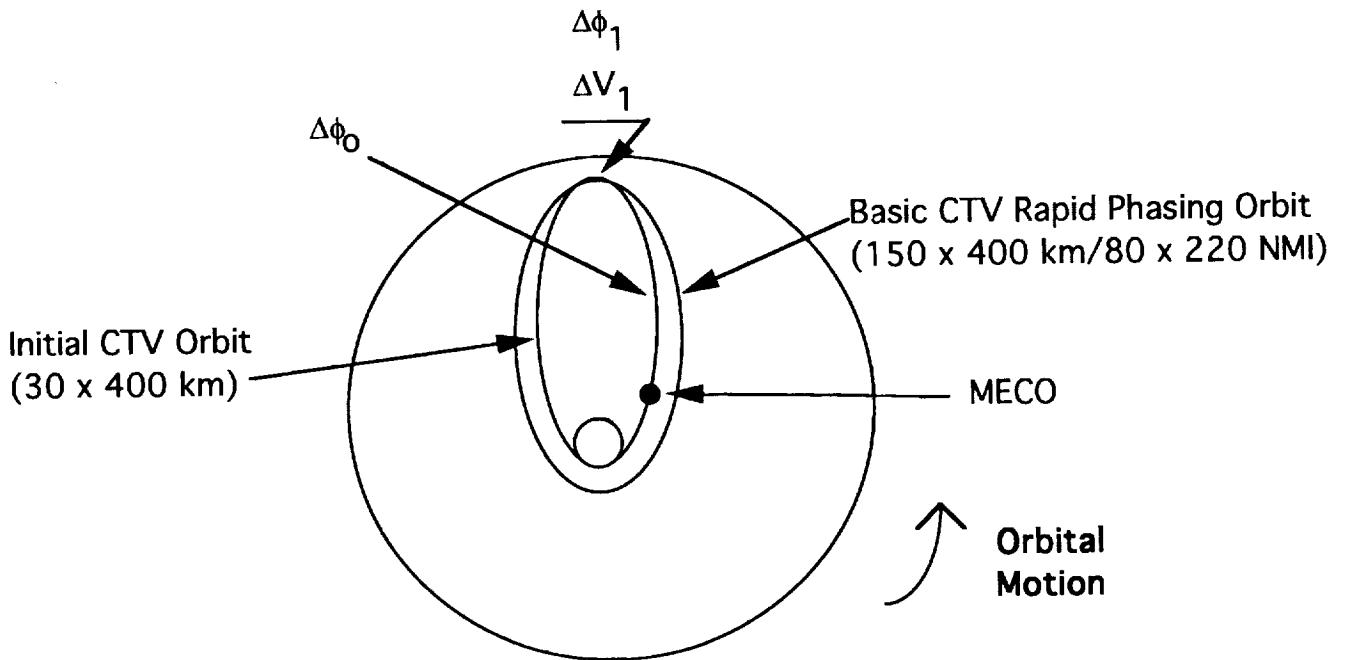
Figure 13. Step 1 of automated spacecraft rendezvous targeting.

MECO of the HLLV core stage and the first burn of the CTV ($\Delta V1$) are illustrated. The angle "$\Delta\phi_o$" (fig. 13) refers to the change in phase relationship between S.S. *Freedom* and CTV which occurs while the CTV travels from MECO to apogee. The burn at apogee raises the CTV/cargo to a minimum acceptable perigee altitude (150 km) (~80 nmi) with S.S. *Freedom* being in a 400×400 km (~220×220 nmi) orbit. Since the semimajor axis of the CTV in the MECO conic (80×400 km) is smaller than that of S.S. *Freedom*, its orbital period will be less and, consequently, it will be closing on S.S. *Freedom*. The angle "$\Delta\phi_1$" refers to the phase catch-up angle for each complete revolution in the rapid phasing orbit (150×400 km) (fig. 13).

The targeting strategy selected for the CTV uses two intermediate phasing orbits prior to executing the first burn of a two-burn SOR maneuver sequence with the first intermediate CTV phasing orbit setting a perigee altitude range of 167 to 241 km (~90 to 130 nmi) with the average being 204 km (~110 nmi) (fig. 14). There will be two revolutions in this orbit prior to raising perigee to the second intermediate phasing orbit. The angle "$\Delta\phi_2$" refers to the phase catch-up angle for two complete revolutions in this orbit. The second intermediate phasing orbit (fig. 15) uses two and one half complete orbits prior to executing the first burn (perigee burn) of the two-burn sequence to a stable orbit 37 km (20 nmi) behind S.S. *Freedom* with the total catch-up phase angle for the two and one half revolutions being shown as "$\Delta\phi_3$". The perigee altitude range is 259 to 333 km (~140 to 180 nmi) with the average being 296 km (160 nmi).

The phase relationship ($\Delta\phi_4$) required at the third perigee passage (two and one half revolutions in second intermediate phasing orbit) for an SOR transfer (165° transfer) which remains free of possible S.S. *Freedom* collision should the second burn fail, is illustrated by figure 16. The value of $\Delta\phi_4$ is a
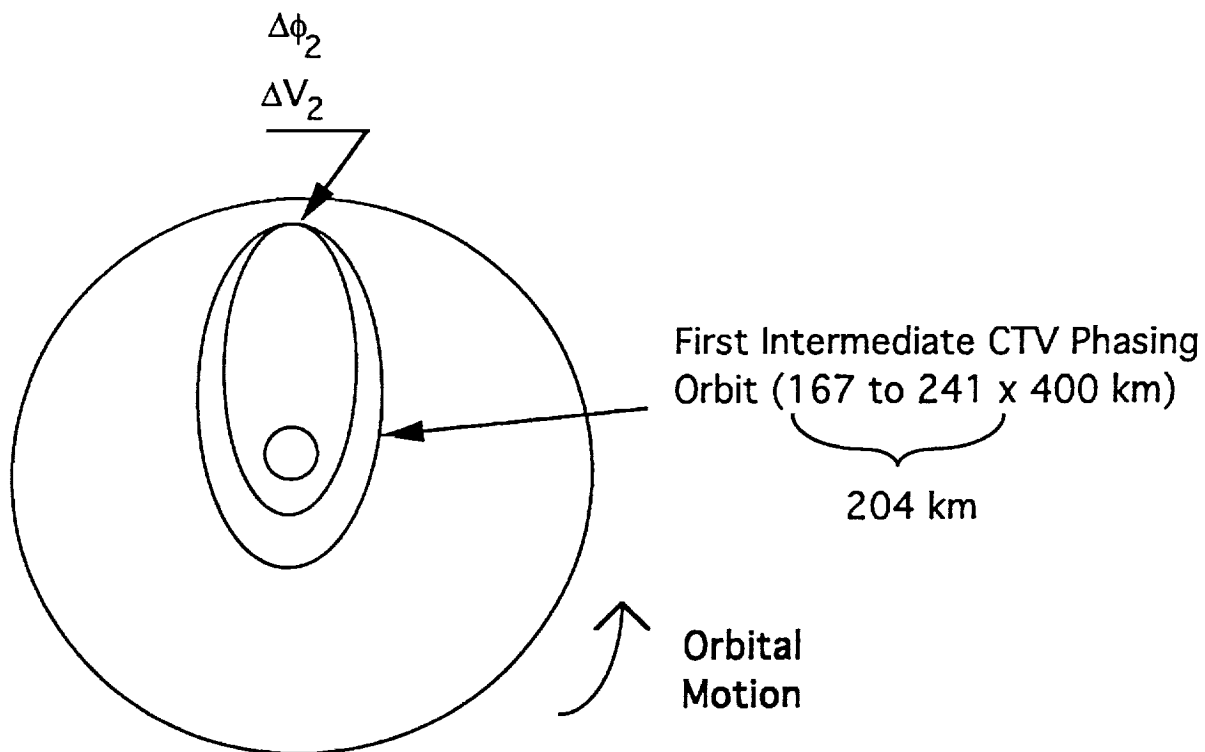
Figure 14. Step 2 of automated spacecraft rendezvous targeting.
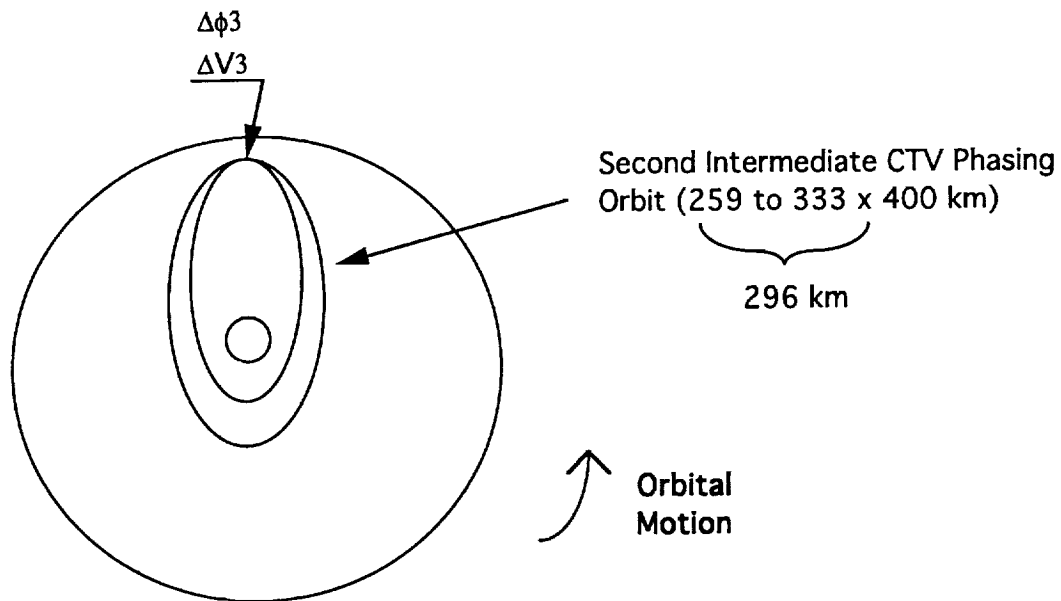
Figure 15. Step 3 of automated spacecraft rendezvous targeting.
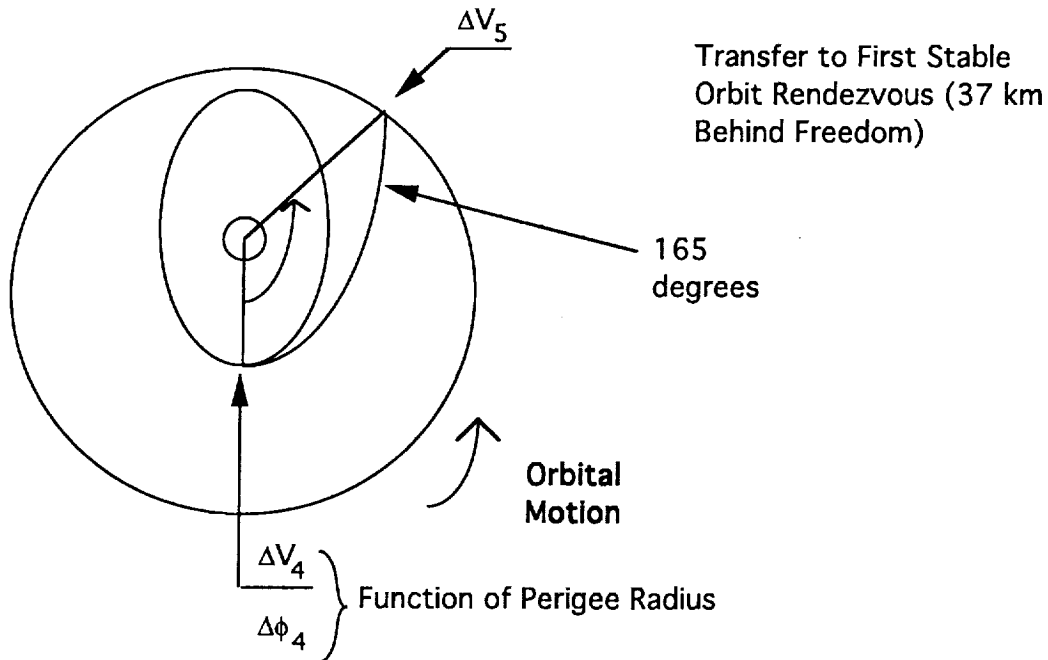
Figure 16. Step 4 of automated spacecraft rendezvous targeting.

function of the perigee radius, but does not vary much for the range of perigee altitudes given (259 to 333 km). This targeting technique is established to allow energy to always be added at each maneuver point and to delay any corrections caused by navigation, modeling error, execution errors, etc., to the next maneuver point. The strategy is always to enforce the desired value of $\Delta\phi_4$ with negligible planar error. The delta velocity penalty for missing the desired "$\Delta\phi_4$" (phase error) is very small as shown by figure 17. The relative motion trajectory which results when the terminal phase of SOR maneuver sequence fails is illustrated by figure 18. It shows a safe approach to and departure from S.S. *Freedom*. The relative motion for an SOR maneuver from 37 to 2 km is shown by figure 19. The relative motion for a SOR maneuver from 2 km to 300 m (proximity capture zone) is illustrated in figure 20. All relative motion trajectories were designed such that, in case of a propulsion failure at the final burn of the SOR sequence of maneuvers, the CTV would always travel away from S.S. *Freedom*.

17
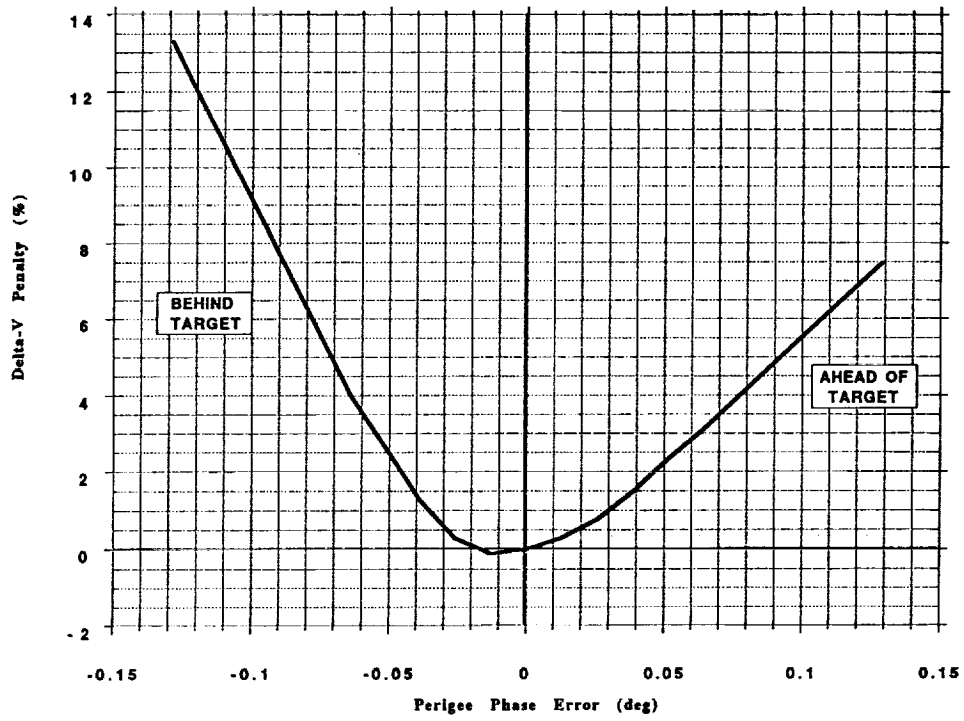
Figure 17. Delta-V penalty versus final phasing error.
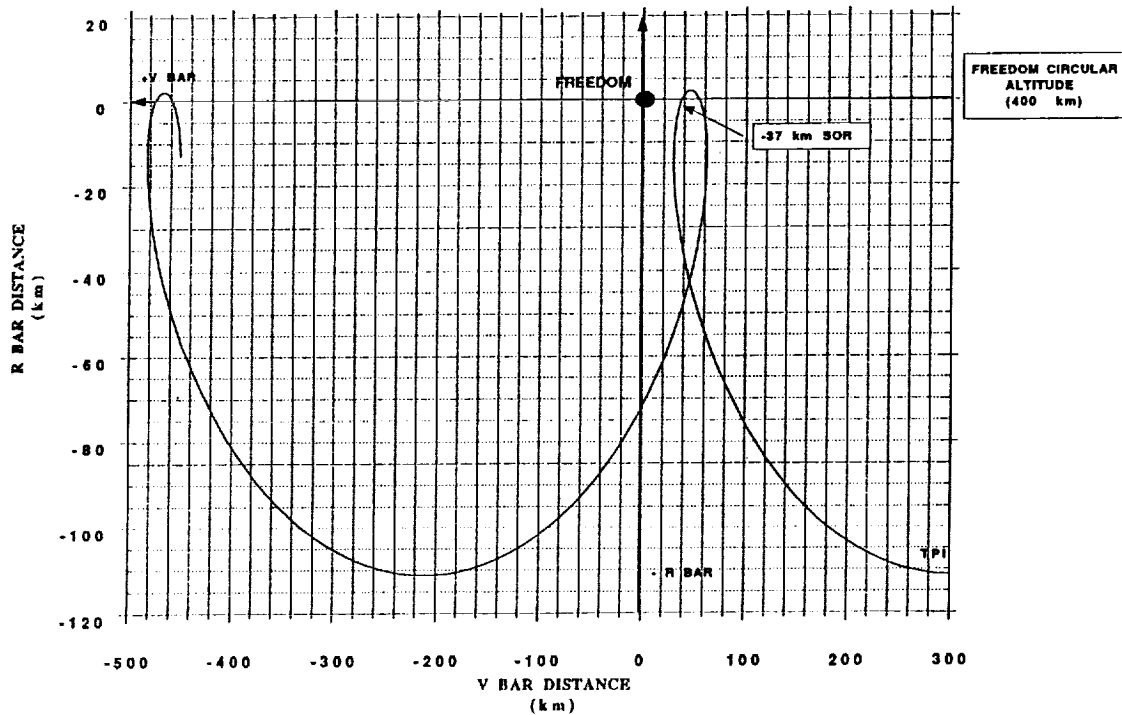
Figure 18. Relative motion plot, failed TPF maneuver on 165° transfer.

18
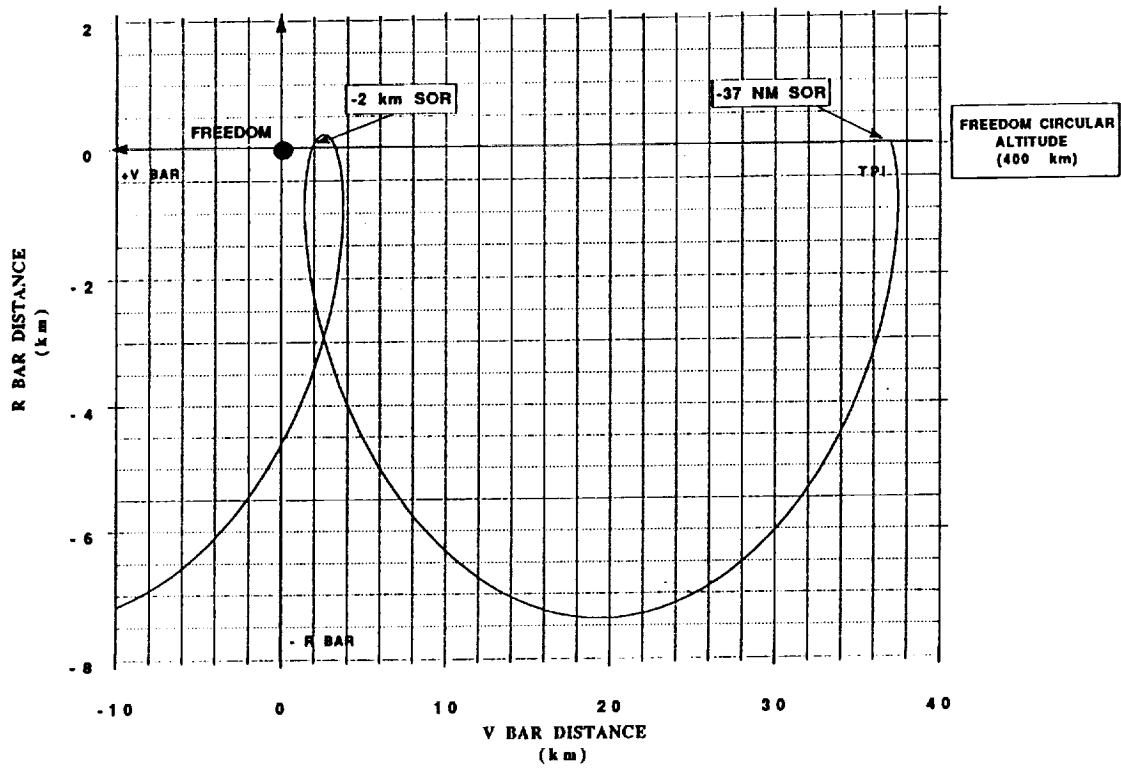
Figure 19. Relative motion plot, failed TPF maneuver on 320° transfer.
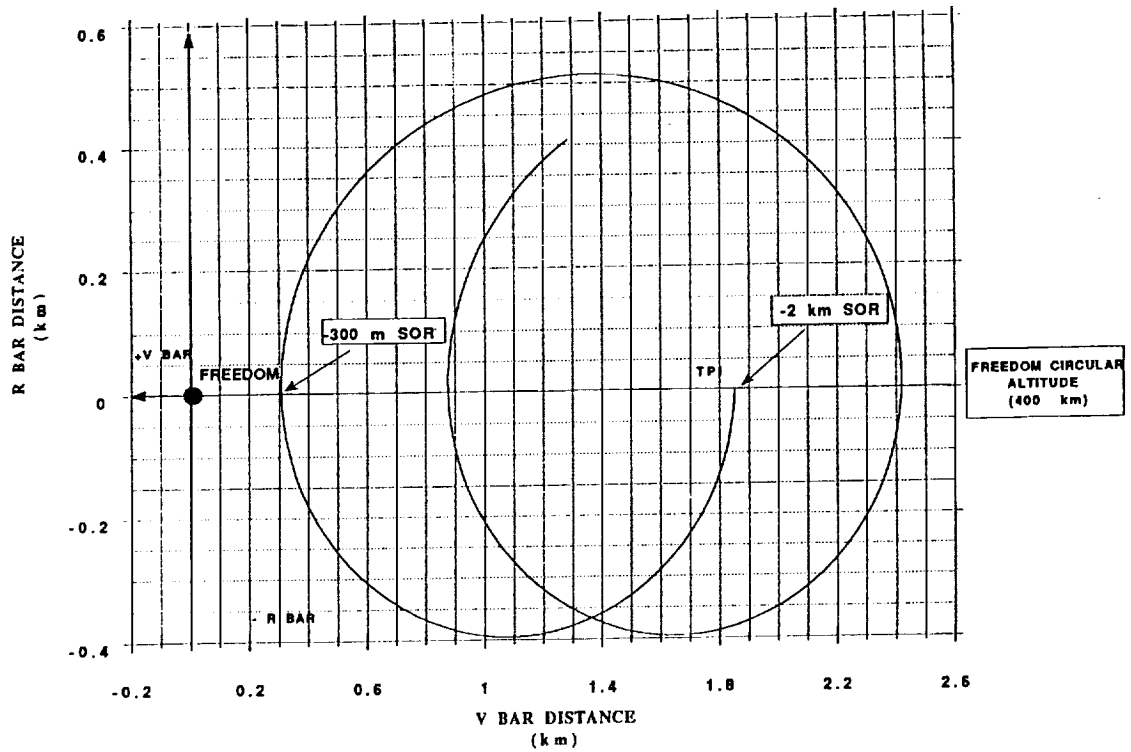
Figure 20. Relative motion plot, transfer from –2 km to –300 m SOR.

The CTV phasing strategy is summarized in figure 21. From the previous discussion, if one takes "$\Delta\phi_0$" and "$\Delta\phi_1$" based upon two revolutions (revs) and the average value of "$\Delta\phi_2$" and "$\Delta\phi_3$," a total catch-up capability of 50.33° can be achieved. If an additional rev (3) is added to the rapid phasing orbit (150×400 km), a total catch-up of 60.60° is possible. The $\Delta\phi$ catch-up harmonics (50.33, 60.60, 70.87, and 81.14°) are illustrated at the bottom of figure 21. Suppose the pursuit/target phase relationship was 53.33° at MECO. The strategy would be to use the 50.33 $\Delta\phi$ harmonic and modify "$\Delta\phi_2$" and "$\Delta\phi_3$" to speed up the phasing (lower perigee from the mean or average value) with the correction ratio being 0.44 to 0.56 for "$\Delta\phi_2$" to "$\Delta\phi_3$" (remember two revs to two and one half revs). For any phasing relationship ($\Delta\phi$) equal to or less than a $\Delta\phi$ harmonics plus one half a delta harmonic (10.27/2°), the smaller $\Delta\phi$ harmonic modified to enforce the desired $\Delta\phi_4$ would be selected. For example, a pursuit/target phase relationship of 59.33° would necessitate using the 60.60° $\Delta\phi$ harmonics modified to slow down the phasing (higher perigee from the mean value). The perigee height versus the number of revs with $\Delta\phi_2$ and $\Delta\phi_3$ phasing is illustrated in the lower right hand side of figure 21.

$\Delta\phi_0$	$\Delta\phi_1$	$\Delta\phi_2$	$\Delta\phi_3$	$\Delta\phi_4$
MECO to Apogee ~ 1900 seconds	Rapid Phasing Orbit ~ 148.2 x 407.4 km (minimum of two revs)	1st Intermediate Phasing Orbit (always two revs) 166.68 km to 240.8 x 407.4 km (AVG 203.7)	2nd Intermediate Phasing Orbit (always 2.5 revs) 259.3 km to 333.4 x 407.4 km (AVG 296.3)	1st Maneuver of Stable Orbit Transfer
~ 2.61 deg +/- 1.0 deg	10.27 deg/rev	13.22 deg to 19.08 deg Range = 5.85 deg AVG = 16.115 deg	7.36 deg to 14.68 deg Range = 7.32 deg AVG = 11.03 deg	A function of Perigee Radius
		Total Range = 13.17 deg		

For 2 revs in 148 x 407.4 km, 2 revs in 203.7 x 407.4 km, 2.5 in 259.3 x 407.4 km, $\Delta\phi=\Delta\phi 0+\Delta\phi1+\Delta\phi2+\Delta\phi3$ = 50.33 deg.
For 3 revs in 148 x 407.4 km, 2 revs in 203.7 x 407.4 km, 2.5 revs in 259.3 x 407.4 km, $\Delta\phi$ = 60.6 deg.
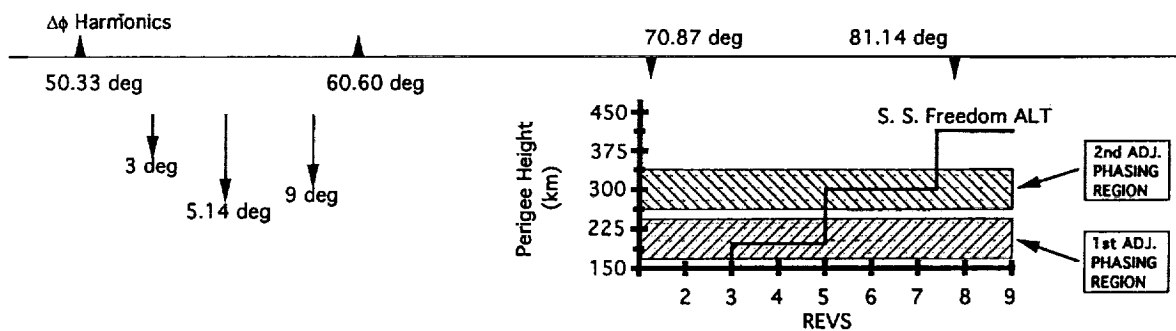
Figure 21. CTV phasing strategy.

The PV rendezvous phasing flight design rules are listed as follows:

Rule 1: There will be a rapid elliptical phasing orbit, an intermediate elliptical phasing orbit that has a lower phasing rate than the rapid phasing orbit, a second intermediate elliptical phasing orbit with lower phasing rate than the first intermediate phasing orbit, a targeted final orbit used for all prior orbital apogee altitudes, and a 165° stable orbit transfer (initiated at the perigee of the second intermediate phasing orbit and completed at S.S. *Freedom's* orbital altitude) consistent with a safe trajectory.

Rule 2: The rapid elliptical phasing orbit shall always have a minimum of two revolutions.

Rule 3: The first intermediate elliptical phasing orbit shall always have two revolutions prior to executing a burn to achieve the second intermediate phasing orbit.

Rule 4: The second intermediate elliptical phasing orbit shall always have two and one-half complete revolutions prior to executing the 165° stable orbit rendezvous maneuver.

Rule 5: The 165° stable orbit rendezvous transfer shall be targeted to a specific location with respect to the target satellite (S.S. *Freedom*) and shall always represent a safe transfer with no danger of target collision within TBD revolutions. The desired phasing relationship of the CTV to the target shall be a function of second intermediate phasing orbit perigee radius magnitude.

Rule 6: Apogee radius of all phasing orbits shall be TBD meters less than the target orbit tangent point.

Rule 7: The range of phasing (catch-up) in both the intermediate phasing orbits (two revs plus two and one-half revs) shall always be 25 percent greater than the phasing available in one revolution in the rapid phasing orbit.

Rule 8: The minimum perigee radius of the first intermediate phasing orbit shall always be greater than the perigee radius of the rapid phasing orbit and equal to the difference between the maximum perigee radius of the first intermediate phasing orbit (slowest catch-up rate of the first intermediate phasing orbit) and the minimum perigee radius of the second intermediate phasing orbit.

Rule 9: The phasing range of the second intermediate phasing orbit shall be 25 percent greater than the phasing range of the first intermediate phasing orbit.

Rule 10: The difference between the maximum perigee radius of the second intermediate phasing orbit and the tangent to the target orbit shall always be four times the difference between the rapid phasing orbit perigee and the minimum perigee of the first intermediate phasing orbit.

Rule 11: The phasing harmonics shall be based upon multiple revolutions in the rapid phasing orbit and the midpoint in the perigee radius range for both the first and second intermediate phasing orbits.

Rule 12: The switch condition from one phasing harmonic to the next shall be based upon the PV phase relationship with the TV being greater than the half-way point between phasing harmonics.

C. An Example Based on Targeting Rules

This example will be based on Keplerian motion, but, for the real algorithm, Earth oblateness and maybe drag effects will need to be modeled in the solution. This set of rules is to determine the sizes of the various PV orbits for adjusting the phasing between the pursuit and TV's. The launch window, planar bias, and targeting based on properly modeling the force on the total system will be described in section V. The TV is assumed to be in a 407.44-km (220-nmi) circular orbit. The rapid phasing orbit selected for this example is a 407.44×148.16-km (220×80-nmi) orbit. The phasing rate (catch-up rate) per revolution (rev) is 10.27°/rev. Rule 7 sets the phase range of the two intermediate phasing orbits to be equal to 12.838° as listed:

$$[\Delta\phi_2+\Delta\phi_3] \text{ range} = 1.25*[\Delta\phi_{RP}] = 1.25*10.27° = 12.84° \ .$$

Rule 9 states that $\Delta\phi_3$ range (second intermediate phasing orbit) shall be 25 percent greater than the $\Delta\phi_2$ range.

$$(\Delta\phi_2+1.25\Delta\phi_2) = 12.84° , \quad \Delta\phi_2 = 5.71° , \text{ and } \Delta\phi_3 = 7.13° \ .$$

The remaining rules state that the spacing between perigee radius of the rapid phasing orbit and the lowest perigee of the first intermediate phasing orbit, the spacing between the highest perigee radius of the first intermediate phasing orbit and the lowest perigee radius of the second intermediate phasing orbit, and the spacing between the highest perigee radius of the second intermediate phasing orbit and the tangent to the target orbit shall be in a ratio of 1:1:4. Determining the intermediate phasing orbits and the spacing between them can be difficult if attempted all in one step. To simplify the procedure, let the perigee radius of the first intermediate phasing orbit be equal to the perigee radius of the rapid phasing orbit (no spacing considered). Two revolutions in this lowest perigee radius orbit give a catch-up angle of 20.54° (2×10.27°). Since the range of catch-up angle is equal to 5.71° ($\Delta\phi_2 = 5.71°$), the catch-up angle per orbit (rev) is (2*10.27−5.71)/2 or 7.42°. Given the catch-up per orbit ($\Delta\phi_{C1} = 7.42°$), the period (time for one complete orbit) can be expressed as follows:

$$TP = (2\pi-\Delta\phi_{C1})*TT/2\pi ,$$

where TT = period of TV orbit.

The semimajor axis then can be expressed as

$$AP = [TP*\sqrt{\mu}/2\pi]^{2/3} = 6,692.049 \text{ km} ,$$

since the apogee radius is equal to the TV circular radius (RAP) in this example, then the perigee radius of the PV in the first intermediate phasing orbit is given as listed:

$$RPP = 2AP-RAP = 6,598.492 \text{ km} \ .$$

The height of perigee is 220.325 km or 118.911 nmi. The range of perigee is 72.165 km (38.966 nmi). Using the same technique, the range of perigee for the second intermediate orbit is likewise 72.165 km. The total spacing between the orbits is 114.950 km (62.068 nmi), giving a spacing between the rapid phasing perigee radius and the first intermediate phasing orbit lowest perigee radius a value of 19.159 km (10.345 nmi). Using a ratio of 1:1:4 for spacing, the following orbits are defined:

I. Rapid phasing orbit—148.16×407.44 km (220×80 nmi)

II. First intermediate phasing orbit—167.32×407.44 km to 239.48×407.44 km (90.345×220 nmi to 129.311×220 nmi)

III. Second intermediate phasing orbit—258.64×407.44 km to 330.81×407.44 km (139.655×220 nmi to 178.621×220 nmi).

To be certain that nothing is lost in this simplifying technique, the following phasing ranges can be computed using these orbits and spacing:

$$\Delta\phi_2 \text{ Range} = 5.70° \text{ (needed } 5.71°) \text{ ,}$$

$$\Delta\phi_3 \text{ Range} = 7.15° \text{ (needed } 7.13°) \text{ .}$$

D. Contingency Rule-Based Targeting

To extend the automated rendezvous concept beyond the primary phasing plan to cover the failure of the propulsion system to execute the intermediate phasing steps, a set of contingency rules needs to be developed. Suppose, for instance, that the propellant line or value had gotten too cold during the long coasting time in the rapid phasing orbit to allow ignition at the first intermediate phasing orbit ignition point. If the problem could be solved on the ground from analysis of the telemetered data, maybe by exposing it to sunlight, the phasing plan could be altered to bypass the second intermediate phasing orbit and use three and one half revolutions in only one orbit to set up the desired phasing at "$\Delta\phi_4$" (SOR transfer point). As an example, suppose the onboard targeting system selects the following mission scenario for rendezvous with a TV in a 407.4 km (220 nmi) circular orbit:

MECO to first apogee—$\Delta\phi_0$	2.61°
Six revs in rapid phasing orbit (148.2×407.4 km) — $\Delta\phi_1$	61.62°
Two revs in first intermediate phasing orbit (222.2×407.4 km) — $\Delta\phi_2$	14.69°
Two and one-half revs in second intermediate orbit (314.8×407.4 km) — $\Delta\phi_3$	9.12°
Total $\Delta\phi$ =	88.12°

Failing to execute the first intermediate phasing orbit transfer and allowing an additional revolution in the rapid phasing orbit would leave 13.62° of phasing to take out in three and one half revolutions ($\Delta\phi_R$ = 88.12°–2.61°–61.12°–10.27° = 13.62°). The period (TP) of the pursuit orbit necessary to take out the remaining $\Delta\phi_R$ (13.62°) is listed:

$$TP = TT-(\Delta\phi_R*TT)/(\text{revs}\times 2\pi) \text{ .}$$

This gives a period of 5,502.66 s and an altitude of perigee of 309.45 km (167.1 nmi). If the problem was solved during the second revolution leaving only two and one half revolutions to take out 3.35° of phasing, the altitude of perigee would be 373.8 km (201.8 nmi). Solving the problem in the third revolution would cause a negative phase angle and result in the logic selecting a circular orbit

above and ahead of the target vehicle, allowing the pursuit vehicle to drift back to the target vehicle prior to executing SOR transfer maneuvers. In a similar manner, should the second intermediate phasing orbit fail to be executed and solved one revolution later, a phase angle of +1.85° would give a perigee height of 376.4 km (203.3 nmi) for the remaining one and one-half revolutions. Obviously, another revolution would cause a switch to above and ahead. A perigee height versus phase angle remaining illustrates this geometry (fig. 22). A typical relative motion plot of the mission is illustrated by figure 23. It should be
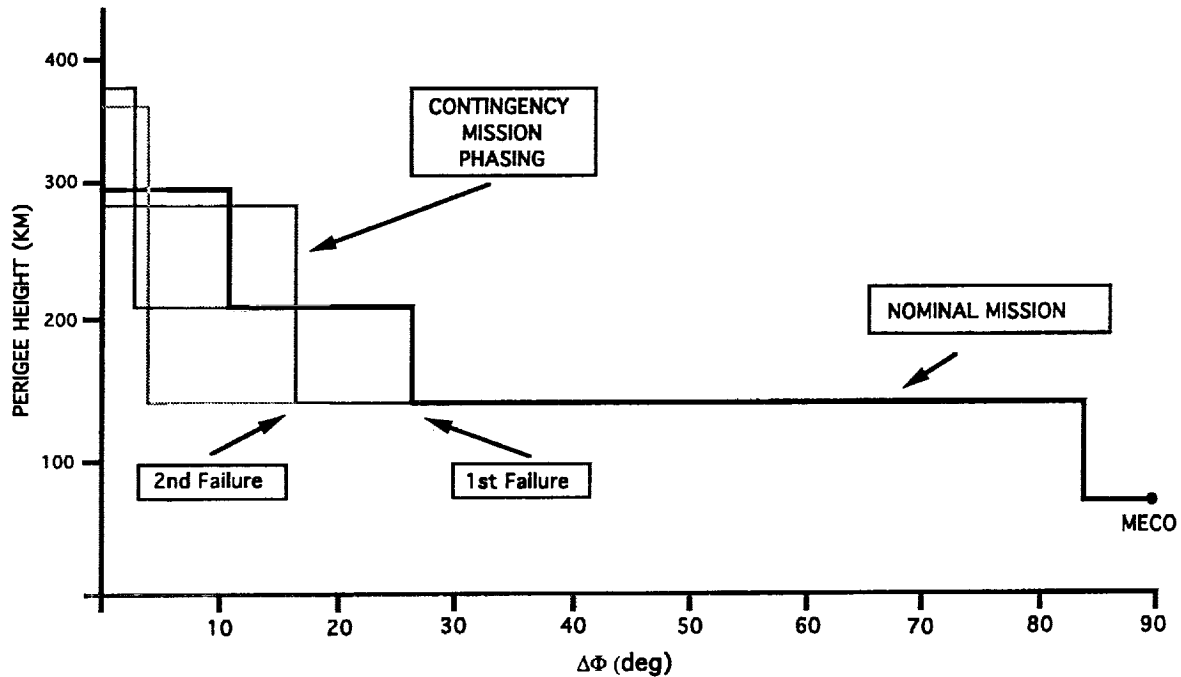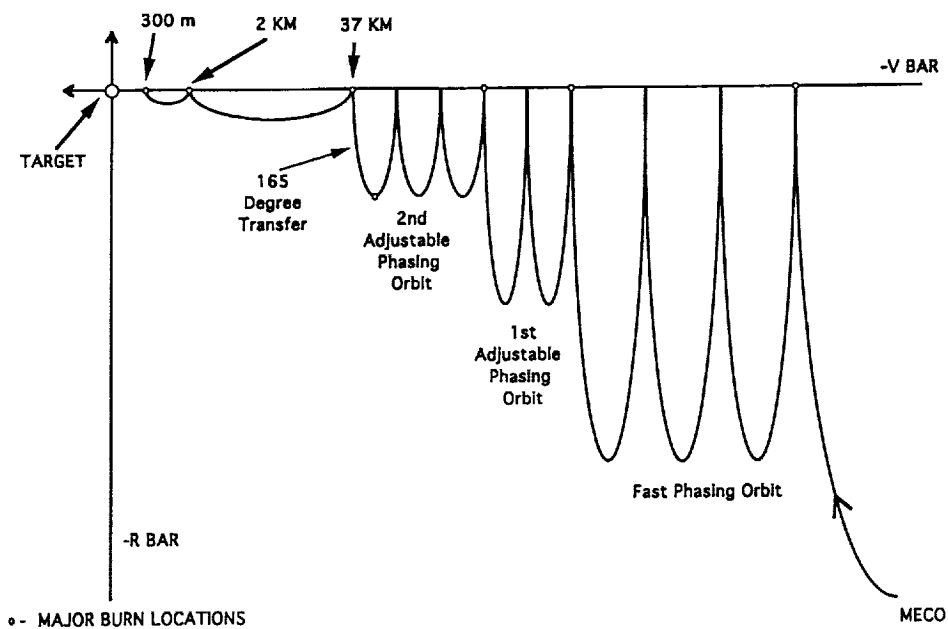
Figure 22. Phase angle remaining to TPI.

Figure 23. Relative motion plot of rendezvous.

24

noted that a failure to execute any of the orbit transfer maneuvers will mean that the PV will be closing too fast and must be slowed down to allow an approach from below and behind. Should the remaining phase angle go negative (pursuit gets ahead of target), the only practical solution is to phase from above and ahead of the TV. The option to phase through 360° would be too costly in time and propellant (differential nodal regression penalty). Although the contingency rules will not be stated in this document, the recovery options are limited and straightforward.

V. PRELAUNCH AND IN-FLIGHT TARGETING STRATEGIES

As stated earlier, it is possible and desirable to decouple the ascent vehicle targeting from the on-orbit automated rendezvous targeting. By creating an orbital insertion surface based upon a fixed orbital inclination and a varying nodal crossing angle around the in-plane (minimum yaw steering) nodal crossing with optimal launch azimuths, the launch window data can be made available to the PV or spacecraft mission planning engineers well ahead of the planned launch date. The launch window data are limited to the established acceptable yaw steering propellant penalty. These data can be tabulated as a function of launch azimuth. The launch window opening and closing times are determined by the PV/TV phase relationships at MECO, the constraints on the PV (mission time, propellant, electrical energy, etc.), and the ascent launch vehicle performance penalty limits.

Given a TV orbital ephemeris, the targeting techniques outlined in section IV and the rule-based targeting of that section can be applied to generate preliminary data using impulsive ΔV's and analytical nodal bias computations as shown by figure 24. The output from the simplified modeling can be used to create finite burns with detailed equations of motion (EOM) to refine the data so that precise (as accurate as the target ephemeris) launch window opening and closing times can be established, nodal bias as a function of phase angle determined (based upon mean perigee radius of first and second intermediate phasing orbits), finite burn guidance targeting data, and contingency targeting generated as well as the launch azimuth versus launch window time function established. Once these data have been generated, the flight computer mission data load can be created for verification analysis. The launch azimuth versus time in the launch window ($AZ = f(TLW)$) determines the ascent vehicle targeting parameters, since these parameters are functions of launch azimuth. The azimuth versus launch window times come from the PV on-orbit targeting which includes the nodal bias compensation and represents the connection between the ascent vehicle and the on-orbit vehicle. This process can be completed months prior to actual launch based upon the best estimate of the TV's orbital parameters. The onorbit targeting can be accomplished as close to the launch window opening as verification allows to get the best data possible and to avoid large on-orbit corrections. A typical HLLV/CTV operational software (S/W) flow is illustrated by figure 25. The mission data load (MDL) update block in the lower middle of the flow represents the update to reflect the latest TV ephemeris (GPS derived).

The in-flight or on-orbit targeting data for automated flight would be minimal with only the nodal bias angle as a function of phase angle, the targeting ephemeris, desired target tangent off-set, and minimum perigee radius of the rapid phasing orbit along with the SOR targeting parameters and prox-imity/collision avoidance maneuver targeting sets being required to complete the rendezvous mission. A flow diagram for illustrating the spacecraft (PV) on-orbit targeting sequence for a rendezvous mission using the rule-based targeting technique is shown by figure 26. The first on-orbit translational ΔV maneuver sequence occurring after MECO (HLLV/CTV flight profile) is the rapid phasing orbit insertion. It is assumed that the CTV global positioning system (GPS) receiver is activated shortly

25

Ascent Vehicle Orbital Insertion Surface

- Determine orbital insertion state and time from lift-off for inplane launch (Minimum yaw steering)

- Determine insertion states for ± nodal variations to the inplane nodal angle within the plane change penalty allocation using optimal flight azimuths

Spacecraft Launch Window Adjustments/Calculations Using Impulsive Δv And Analytical Computations

- Determine lift-off time for inplane alignment
- Nodal bias computations
- Launch window(LW) opening/ closing based upon mission time/propellant/electrical energy constraints
- ΔV events timeline for max mission time
- Launch azimuth(Az) variation with time in launch window

Finite Burn and EOM Modeling

- Finite burn trajectories
- LW open/close
- Guidance targeting data
- Contingency targeting data
- Az = f(launch window time)

MDL Verification

Guidance and Targeting Mission Data Load(MDL)

Figure 24. Spacecraft automated rendezvous flight design software.

OWG: Operational REOTS
HDO,MSFC,SSF,JPO,JSC,Contr.

NLS Projects Office: Program REOTS
MSFC,IIDO,JPO

IWG: Interface REOTS
IIDO,MSFC,SSF,JPO,JSC,Contr.

HLLV/CTV Flight Vehicle REOTS for Development of Operational Trajectories and MDL Parameters for Operational Flight S/W (OFS) and Contingency Uplink/Commands/Data
MSFC/Contractor/JPO

CTV Operational Trajectories
1) Phase Window Analysis (HLLV Hand-Off)
2) Contingency Analysis/Plans
3) Engineering Analysis
4) Baseline MDL Files Generated from Engineering Disciplines (Launch minus 3 Months)
MSFC/Contractor

MDL Verification
1) Non Realtime S/W Stress Test of MDL Files Using OFS Equivalent S/W
2) Produce Verification Test Report
3) Create Flt. Computer Onboard Flt. S/W (OBFS) Tape (OBFS+OFS+MDL)
MSFC/Contractor

MDL Validation
1) S/W Integration Lab (SIL)
2) Produce Validated Tape and Test Report (Complete L-1 Month)
MSFC/Contractor

HLLV Operational Trajectories
1) Launch Window Analysis
2) Contingency Analysis/Plans
3) Engineering Analysis
4) Baseline MDL files Generated from Engineering disciplines (Launch Minus 3 Months)
MSFC/Contractor

MDL Update
Mission Specific Data Load (MSDL) (L-1 Month/Later)
MSFC/Contractor

Special Documentation
1) Mission Rules
2) Operational Plans
3) Training Plans
4) Cargo Manifest Plans
5) etc.
MSFC,IIDO,SSF,JPO,JSC,Contr.

Validate Flight Tape
KSC/MSFC Contr.

Post Flight Eval.
MSFC/Contr.

HLLV/CIV Integration
KSC

HLLV/CIV/Cargo S/W Testing
KSC/MSFC/Contractor

HLLV/CTV Flight System Monitor/Flight Control Functions (MSDL Updates)

MAIN FLOW
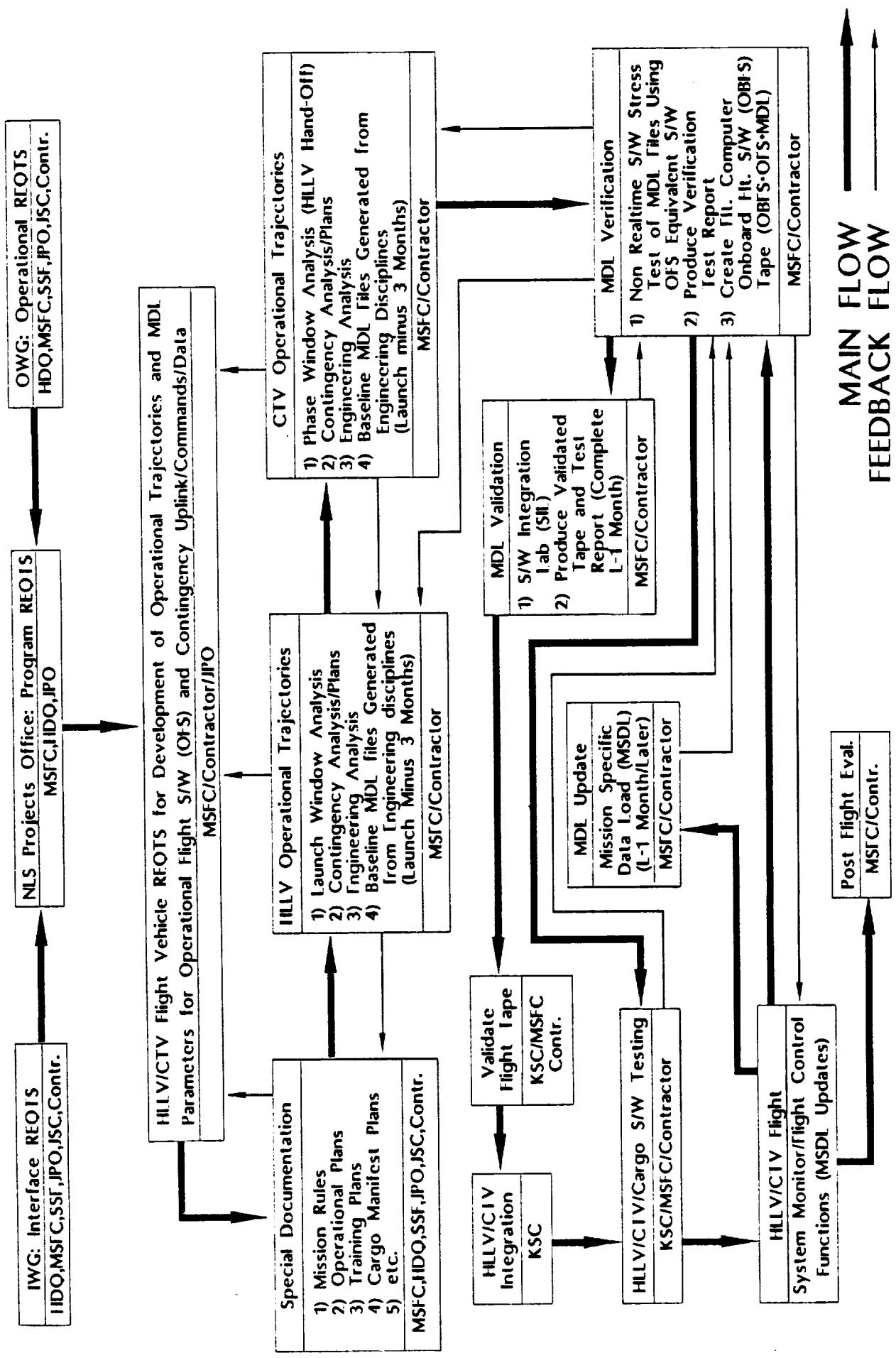FEEDBACK FLOW

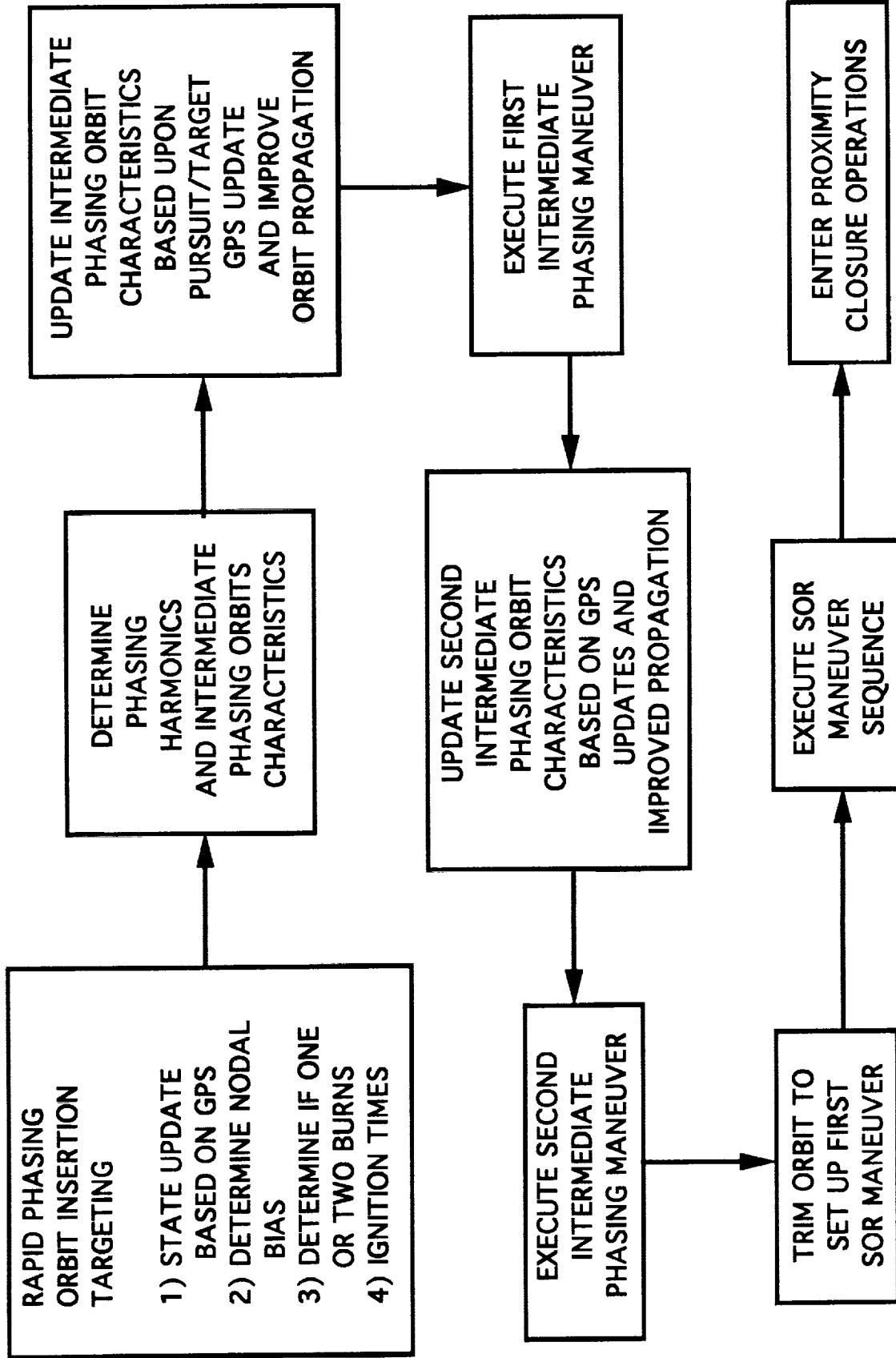Figure 25. HLLV/CTV operational S/W flow.

27

Figure 26. Spacecraft on-orbit targeting sequence for rendezvous.

after MECO. With a precise PV navigation state and a precise TV state available, GPS-derived and bent-piped to pursuit through the telecommunications and data relay satellite (TDRS) system, the phase angle at apogee can be determined as well as the required nodal bias. Studies have shown that the perturbed state at MECO can cause a two-burn maneuver sequence to be required to achieve the desired rapid phasing orbit. Large dispersions in the MECO conic (apogee and orbital planes) are best corrected by an optimal two-burn sequence.

Once in the rapid phasing orbit, the phasing harmonics can be computed using the flight computer algorithms to determine the intermediate (first and second) phasing orbits with updates as better navigation states, and the orbit propagation error is reduced as the required propagation time is reduced. All rapid phasing errors are deferred to the first intermediate phasing orbit and split by the 0.444 to 0.556 ratio. Once the first intermediate phasing orbit has been executed, any phasing/planar errors are deferred to the second intermediate phasing orbit. Once in the second intermediate phasing orbit, orbital trims to enforce the desired conditions at the first burn of the SOR point are executed at each apogee passage when the ΔV exceeds a threshold value. Once in the SOR orbit, proximity closure to the target can proceed on command from the ground or from the space station, if it is a S.S. *Freedom* resupply mission.

VI. CONCLUSIONS

Based upon the level of technology available today, such as global positioning system receivers/processors, fast and efficient flight computers, and advanced software design and compilers, it is possible to achieve automated spacecraft rendezvous with limited automated contingency recovery that minimizes operational cost. The approach described in this document explains how the ascent vehicle targeting and flight design can be decoupled from the on-orbit spacecraft targeting and how the automated system continually improves the process as time advances in the mission. The concept continually adds energy to the system to reduce the performance penalty. This approach allows software verification and validation to take place well in advance of the scheduled launch date with refinements to the mission data load possible on the day of launch.

Techniques similar to this would be possible for manned or unmanned launches from the surface of Mars in which a rendezvous with a return to Earth spaceship is required without help from Earth-based systems. A constellation of Mars navigation satellites (maybe 8 to 10) could provide the navigation accuracy required (not as accurate as Earth GPS) with long distance ranging devices for terminal rendezvous control.

REFERENCES

1. Deaton, A.W., Upadhyay, T.N., and Catterill, S.: "Autonomous GPS/INS Navigation Experiment for Space Transfer Vehicle (STV)." First European Space International Conference on Spacecraft Guidance, Navigation, and Control Systems, Noordwijk, The Netherlands, June 4, 1991.

2. Deaton, A.W., Upadhyay, T.N., and Catterill, S.: "Autonomous Reconfigurable GPS/INS Navigation and Pointing System for Rendezvous and Docking." AIAA Space Programs and Technologies Conference, Huntsville, AL, March 24, 1992.

3. Deaton, A.W., and Brandon, P.D.: "Development and Applications of an Orbital Insertion Surface for the Space Shuttle Orbiter/Tug." NASA TM X-64715, January 10, 1973.

4. Raushe, K.H.: "The Cargo Transfer Vehicle." AIAA 92-1650, AIAA Space Programs and Technologies Conference, March 24–27, 1992, Huntsville, Alabama.

5. Brauer, G.L., Cornick, D.E., Olson, D.W., Petersen, F.M., and Stevenson, R.: "Program to Optimize Simulated Trajectories (POST)." Volume II Utilization Manual, Martin Marietta Corporation, September 19, 1989.

APPENDIX A

Example Autonomous CTV/S.S. *Freedom* Rendezvous Mission

The purpose of this appendix is to illustrate the methods involved in determining the mission profile for a Space Station *Freedom* (S.S. *Freedom*) rendezvous mission using the cargo transfer vehicle (CTV). The problem posed here is the calculation of a daily launch window over a 5 consecutive day time span for the heavy lift launch vehicle (HLLV) to put the CTV into an orbit to rendezvous with the S.S. *Freedom*, subject to the restrictions that the launch window on any given day is at least 30 min in length and the payload penalty due to launching on a nonoptimum azimuth does not exceed 2,500 lb.

The information obtained from this analysis will include: optimum launch date, launch window open/close time, mission duration, phasing altitudes and revolutions, and payload penalty for yaw steering.

The upper half of table A1 contains an example S.S. *Freedom* state vector at a more or less arbitrary initial time. The state vector for CTV at MECO that corresponds to an in-plane launch (azimuth = 90°) is also listed, and is referenced to an Earth-fixed coordinate system. Once the space station's state vector is provided, the time of the in-plane condition for any day can be calculated using the method discussed in section III. The S.S. *Freedom*'s state vector can then be propagated to the first in-plane launch opportunity to yield the state vector listed in the lower half of table A1. The time of the in-plane opportunity can be used to convert the CTV Earth fixed MECO state vector to an inertial state vector. The relative phase angle between the space station and CTV can then be calculated. Table A2 is a tabulation of 5 consecutive days of the in-plane launch opportunities and their respective relative space station/CTV phase angle at MECO. This procedure can be done for as many days as desired.

The previous paragraph describes in-plane launch opportunities which occur at one instant of time each day. A launch window is a finite interval of time on either side of the in-plane instant. It necessarily involves launching at times that will not produce orbits which are in-plane with the S.S. *Freedom* if a due east launch azimuth is used. Trajectories with azimuths other than due east will be required to get into the same plane with the S.S. *Freedom* and these will be less than optimal. The ascent profile of these trajectories must be shaped such that at MECO their ascending nodes will match that of the S.S. *Freedom*'s orbit plane. This requires an optimization procedure to determine the best launch azimuth and best MECO values of true anomaly and argument of perigee for each launch time across the launch window. This set of best values of launch azimuth and best MECO values of true anomaly and argument of perigee as a function of time from the in-plane opportunity is called an insertion surface. In the example problem to be shown here, the program POST was used to generate this surface.

The phasing strategy, and rule-base targeting methodology discussed in section IV can be used to generate the number of rapid phasing orbits and the respective mission times for the range of possible phase angles between the CTV and space station at MECO. Figure A1 is a plot of mission time versus all possible phase angles at MECO. The stairstep shape of this graph is caused by the addition of a revolution in the rapid phasing orbit. Each time another revolution in the rapid phasing orbit is required the mission time will increase at the rate of the orbital period of the rapid phasing orbit (about 1.5 h). If the rule-based targeting methodology is used, assuming a space station altitude of 407.44 km and a minimum rapid phasing orbit perigee altitude of 148.16 km, the ranges of perigee altitudes for the two adjustable phasing orbits, can be calculated (table A3).

As time increases beyond the launch window opening, the relative phase angle between the space station and CTV at MECO will increase. When the relative phase angle at MECO is a $\Delta\phi$ harmonic, the perigee altitudes of the adjustable phase orbits are in the middle of their corresponding ranges. As the

31

relative phase angle increases beyond the $\Delta\phi$ harmonic, the perigee altitudes of the adjustable phase orbits will decrease (increasing the catch-up rate). At midway between the $\Delta\phi$ harmonics the adjustable orbit perigee altitudes are at the minimum of their ranges. If additional revolutions are required in the rapid phasing orbits, the perigee altitudes of the two adjustable orbits will jump to their maximum altitudes to enforce the 2 revolutions + 2.5 revolutions rule and assure the proper angle at the stable orbit rendezvous point. Figures A2 and A3 show how the first and second adjustable orbit perigee altitudes vary with the relative phase angle between space station and CTV at MECO. In section IV B, the $\Delta\phi$ harmonics are listed as 50.33°, 60.60°, 70.87°, etc. It can be seen from figure A4 that at a 70.87° relative phase angle at MECO, the adjustable orbit perigee altitudes are in the middle of their ranges. As the phase angle moves from 70.87° to 76.01° the adjustable orbits perigee altitudes move from the nominal to the minimum of their ranges. This gives a greater catch-up rate to account for the greater phase angle than the nominal harmonic. Once the phase angle reaches a halfway point between the two harmonics, the mission time jumps 1.5 h as the adjustable orbit perigee altitudes move from the minimum value of their range to the maximum value (fig. A4).

The program POST was used to generate the yaw steering payload penalty across the launch window for the HLLV. The penalty was generated for the range of launch times from 60 min early to 45 min late based on the in-plane launch. Two criteria dictate the selection of launch window: maximum yaw steering penalty for launch vehicle, and a minimum launch window time. For the following example, the criteria were a 2,500-lb maximum yaw steering payload penalty and a minimum 30-min launch window. If these criteria are used, a 49.4-h maximum mission time (based on the worst case phase relationship that still allows a 30-min launch window) can be calculated. Using the minimum number of revolutions in all orbits a minimum mission time of 10.23 h can be calculated.

If the mission time (for a specific in-plane launch phase angle between the space station and CTV at MECO) is plotted on the same curve as the yaw steering penalty, a plot similar to figure A5 will be generated. The 1.75-min early launch will yield a mission time of 10.23 h and a yaw steering penalty of almost zero. The 36-min late launch will yield a mission time of 31.3 h and the maximum yaw steering penalty of 2,500 lb. It should be noted that when selecting the launch window, the entire launch window lies on one side or the other of the 360° phasing point. The launch window for this particular relative phase angle between CTV and space station would yield a 37.75-min launch window. Using table A3 and the in-plane phase relationship for this case of 57.25°, the perigee altitudes of the two adjustable phasing orbits can be calculated for the in-plane launch condition. Since the phase angle lies between the $\Delta\phi$ harmonic of 50.33° and 60.60°, the switch point for another revolution will occur at 55.465°. This means that 3 revolutions in the rapid phasing orbit will be required. The adjustable orbit perigee altitudes can then be calculated to be 227.9 and 320.5 km. The same type of calculation could be used for any launch time within the launch window.

Figure A6 shows the launch window data based on the phase angle for the next in-plane launch opportunity from table A2. It can be seen from figure A6 that the launch window will open at 23.1 min before, and close at 36 min after the in-plane condition. The 23.1-min early launch would have a mission time of 10.23 h and a yaw steering penalty of 119.7 lb. The 36-min late launch would have a mission time of 43.5 h and the maximum yaw steering penalty of 2,500 lb. The total launch window available would be 59.1 min.

Figure A7 shows a plot of the data for the third day in-plane launch opportunity. The launch window should open at 44.7 min before and close at 25.6 min after the in-plane launch opportunity. At 44.7 min early, the yaw steering penalty would be 2,056 lb with a mission time of 10.23 h, and the 25.6-min late launch would yield a yaw steering penalty of 1,081 lb with the maximum mission time of 49.4 h. The total launch window available would be 70.3 min.

Figure A8 shows a launch window that would open at 47.8 min before and close at 4 min after the in-plane launch opportunity. The 47.8-min early launch would yield the 2,500-lb maximum yaw steering penalty limit with a mission time of 20.8 h. The 4-min late launch would yield a yaw steering penalty of 17 lb and the maximum mission time of 49.4 h. The total launch window available would be 51.8 min.

Figure A9 shows a launch window that would open at 5 min after the in-plane launch opportunity with a mission time of 10.23 h and a yaw steering penalty of 29.9 lb. The launch window would close at 36 min after the in-plane launch opportunity with a mission time of 28.37 h and the maximum yaw steering penalty of 2,500 lb. The total launch window available would be 41 min.

It can be seen by the previous example that as consecutive launch opportunities are examined a pattern appears. Depending on the orbital altitude of the space station, the in-plane launch time will change by a constant amount from day to day. This is true as well for the relative phase angle change between space station and CTV that occurs for consecutive days. If a minimum mission time and yaw steering penalty is desired, an optimum in-plane launch opportunity MECO phase angle can be calculated. Using the orbital rate of the space station (about 3.88° of phase per minute of launch window) a launch window that opens at 20 min before the in-plane launch condition and closes at 10 min after the in-plane launch opportunity, will yield the minimum yaw steering penalty due to the nonsymmetric nature of the yaw steering payload penalty curve. If the opening of the window corresponds to a minimum mission time of 10.23 h, the first harmonic of the phasing strategy discussed in section IV B of 50.33° (minimum number of revolutions in each of the phasing orbits) must be the phase angle at that point. Using the space station's orbital rate and the 20-min early launch window time, the optimum relative phase angle between space station and CTV at MECO, for the in-plane launch condition, can be found to be 127.93°. The 10-min late launch would have a mission time of 27.23 h. The yaw steering penalty for both the open and close of the window would be 81.2 lb.

If it is desired to select a launch date and time that corresponds to the minimum mission time and minimum yaw steering payload penalty, then a relative phase angle at MECO of 127.93° should be selected. A table such as table A2 can be generated for a number of days and a phase angle which is close to the 127.93° can be found. As the orbital altitude of the space station varies (90-day cycle) these calculations would have to be adjusted.

The same method can be used to determine the maximum mission time for the worst phase relationship between the space station and CTV at MECO. The limiting value of the yaw steering penalty (which is 2,500 lb and occurs at 36 min after the in-plane launch condition) and the requirement that the entire launch window lie on one side or the other of the 360° phasing condition, will yield the condition of the minimum $\Delta\phi$ harmonic of 50.33° occurring later than 7 min after the in-plane launch condition. This, coupled with the minimum 30-min launch window, will force the opening of the launch window to be chosen at the 47.8-min early launch time (2,500 lb yaw steering penalty limit). If the calculations are performed for this case, a minimum phase angle at MECO of 19.29° is obtained. The opening of the launch window will then have to be chosen at the 47.8 min early time and close at 17.8 min before the in-plane launch with a maximum mission time of 49.4 h.

The optimization of orbit transfers by the CTV requires that the CTV does not perform any out-of-plane burns. To account for the difference in nodal regressions of the CTV and space station's orbital planes, a correction to launch time can be performed so that only dispersions have to be corrected. For very long mission times, the difference in nodal regression between the CTV and space station's planes can be quite large. Figure A10 shows a plot of the differential nodal regression between the two planes as a function of relative phase angle at MECO. The correction to launch time based on the relative phase angle at MECO is also plotted on figure A10. The discontinuity of the nodal regression function at the

360° phasing point is another reason why the full launch window must lie on one side or the other of the 360° phasing condition. The targeting algorithm used by the ascent vehicle will target to the same Earth fixed state vector as was calculated without nodal regression of the planes but the actual launch time will be biased by the time required to rotate the two planes using the Earth's rotational rate. An example of this can be seen by using a relative phase angle at MECO of 180° as follows:

If the relative phase angle between the CTV and space station at MECO is 180°, the mission time for this condition would be 29.9 h. It can be seen from figure A10 that a nodal bias of 0.545° would have to be corrected for by launching the ascent vehicle 2.18 min prior to the calculated time.

This example may help to understand the rendezvous problem but it does not include many of the refinements required in the actual targeting algorithm. Refinements include: change of argument of latitude across the launch window, inclusion of the $\Delta\phi$ required to perform the 165° transfer to the stable orbit rendezvous point, and apsidal rotation during the mission.

Table A1. Space Station *Freedom* state vector.

Example State Vector of Space Station Freedom Valid at 1/23/1999 GMT 5.9 hrs

Semi Major Axis	6787485 meters
Eccentricity	0.0008185686
Inclination	28.35 deg
Argument of Perigee	105.85 deg
Right Asc. of Node	277.78 deg
Mean Anomaly	26.238 deg

State Vector of CTV at MECO (azm = 90°)

Semi Major Axis	6610689.5 meters
Eccentricity	0.026471
Inclination	28.35 deg
Argument of Perigee	57.53 deg
Longitude of Asc. Node	189.04 deg
True Anomaly	44.54 deg

Inplane Launch Condition State Vectors At 1/23/1999 GMT 21.43 hrs

Space Station

Semi Major Axis	6789349.9 meters
Eccentricity	0.0008707125
Inclination	28.35 deg
Argument of Perigee	140.0643deg
Right Asc. of Node	273.22553 deg
Mean Anomaly	18.48 deg

CTV (at MECO)

Semi Major Axis	6610689.5 meters
Eccentricity	0.026471
Inclination	28.35 deg
Argument of Perigee	57.53 deg
Right Asc. of Node	273.22553 deg
Mean Anomaly	44.54 deg

*NOTE : Osculating Orbital Elements
        Relative to Coordinate System fixed with Aries

35

Table A2. In-plane launch times and data.

Inplane LaunchTime (Jan. 1999)		CTV Arg. of Lat. (deg)	SSF Arg. of Lat. (deg)	Relative Phase of SSF/CTV at MECO (deg)
Day	GMT hr			
23	21.43	102.07	159.321	57.251
24	20.91	102.07	242.444	140.374
25	20.38	102.07	325.708	223.638
26	19.86	102.07	48.959	306.889
27	19.33	102.07	132.314	30.244

Table A3. Adjustable orbits perigee altitude ranges.

	Maximum (km)	Nominal (km)	Minimum (km)
1st Adj. Orbit	240.8	203.7	166.7
2nd Adj. Orbit	333.4	296.3	259.3
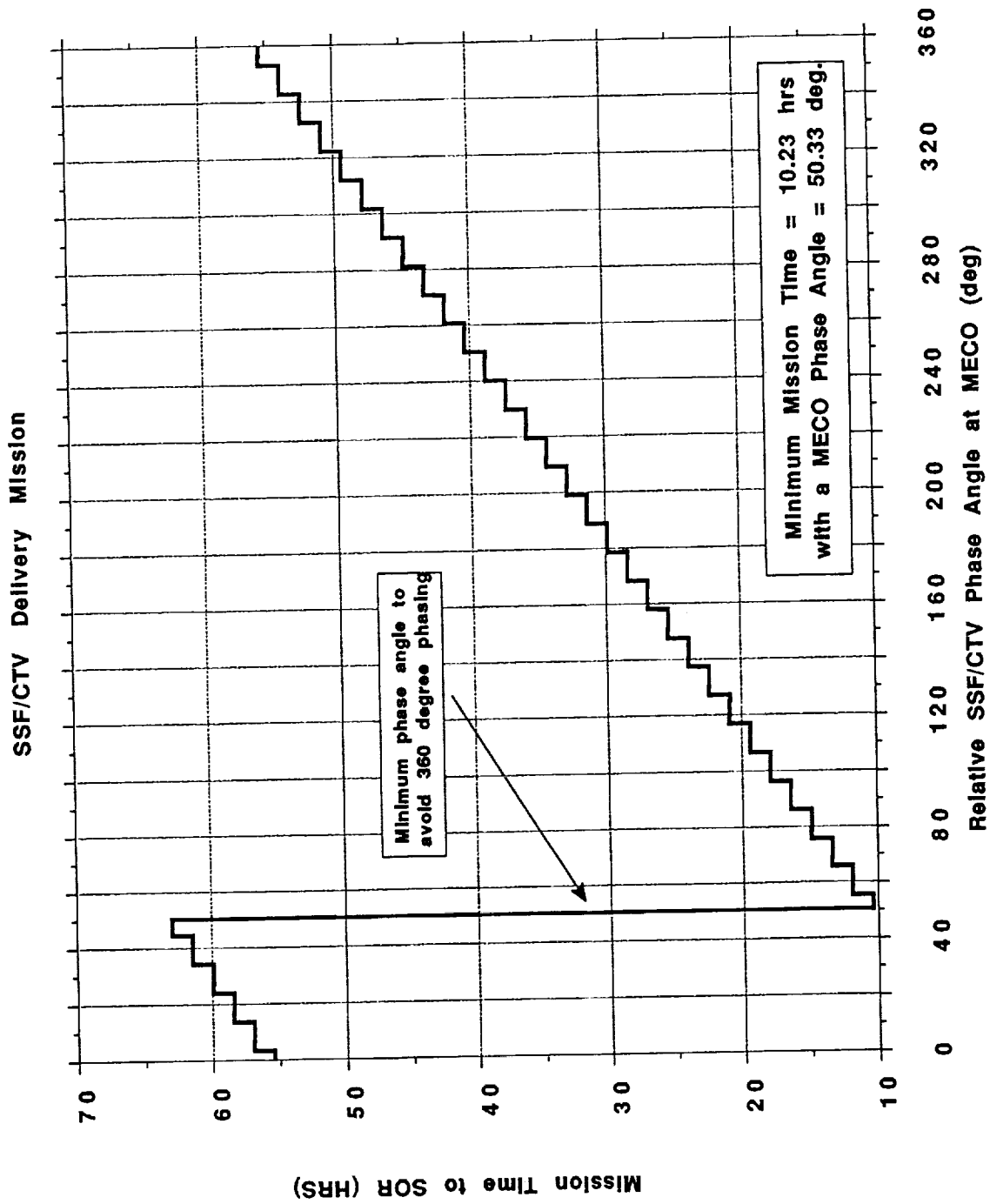
Figure A1. Mission time to SOR.
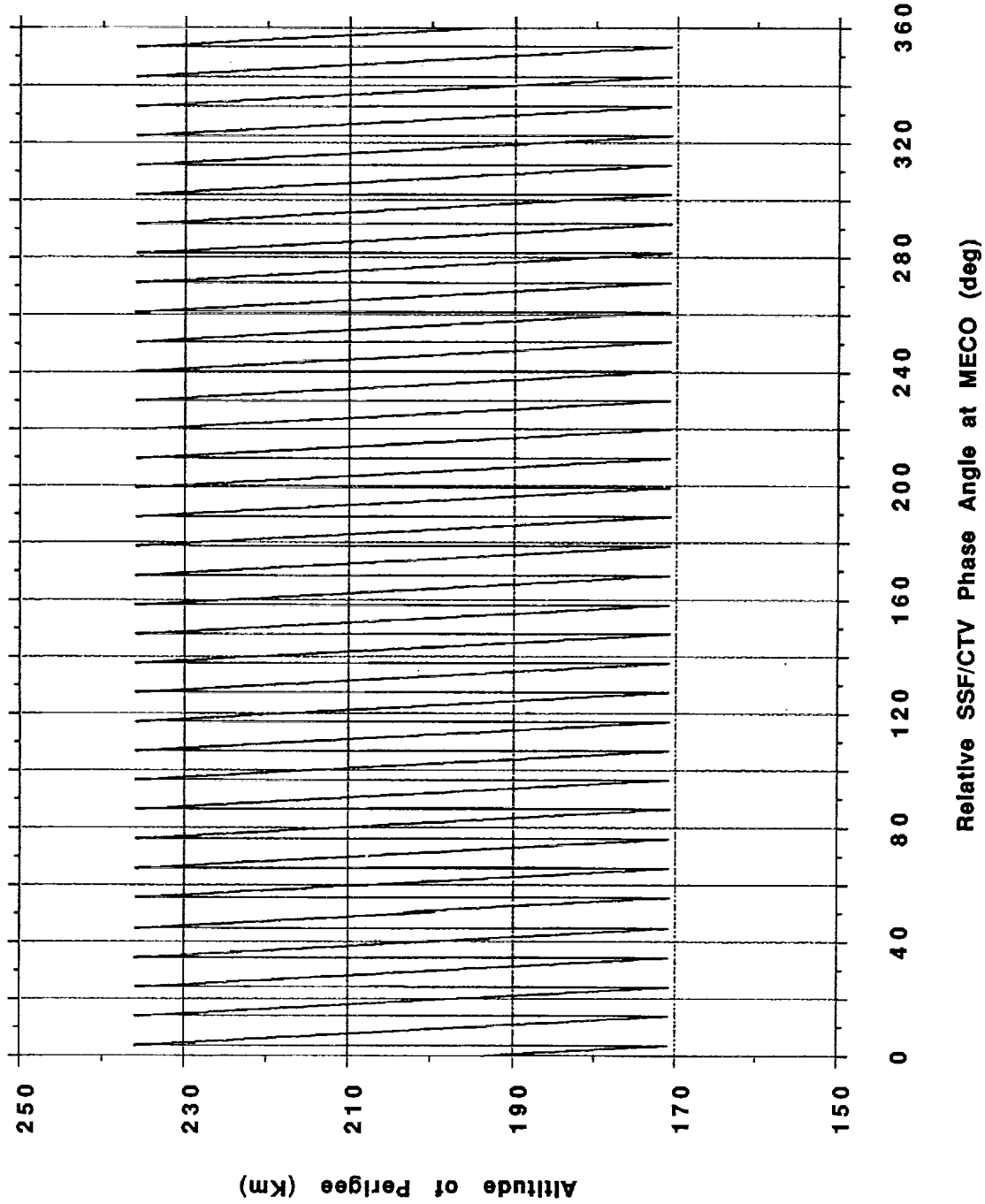
Figure A2. Perigee altitude of first adjustable phasing orbit.
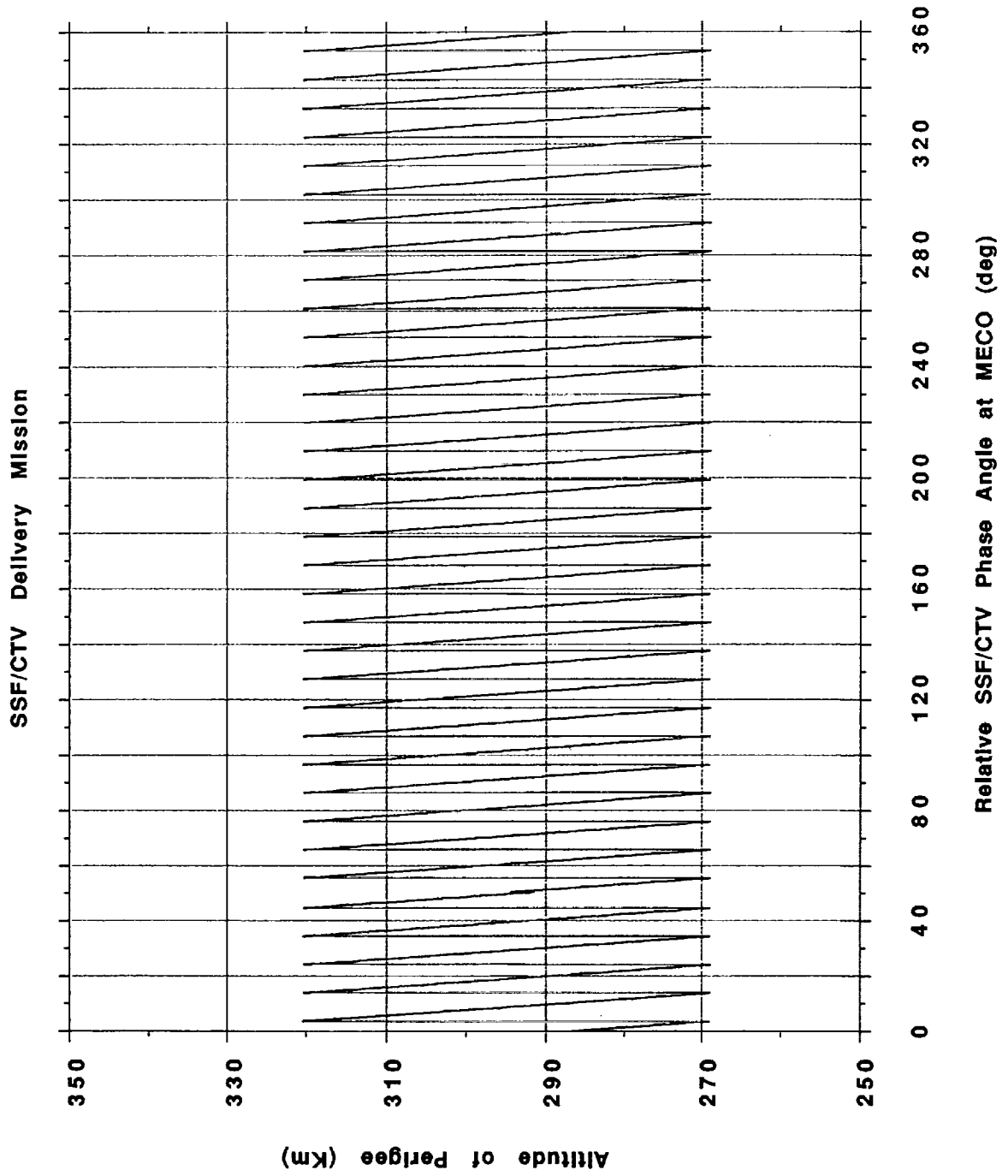
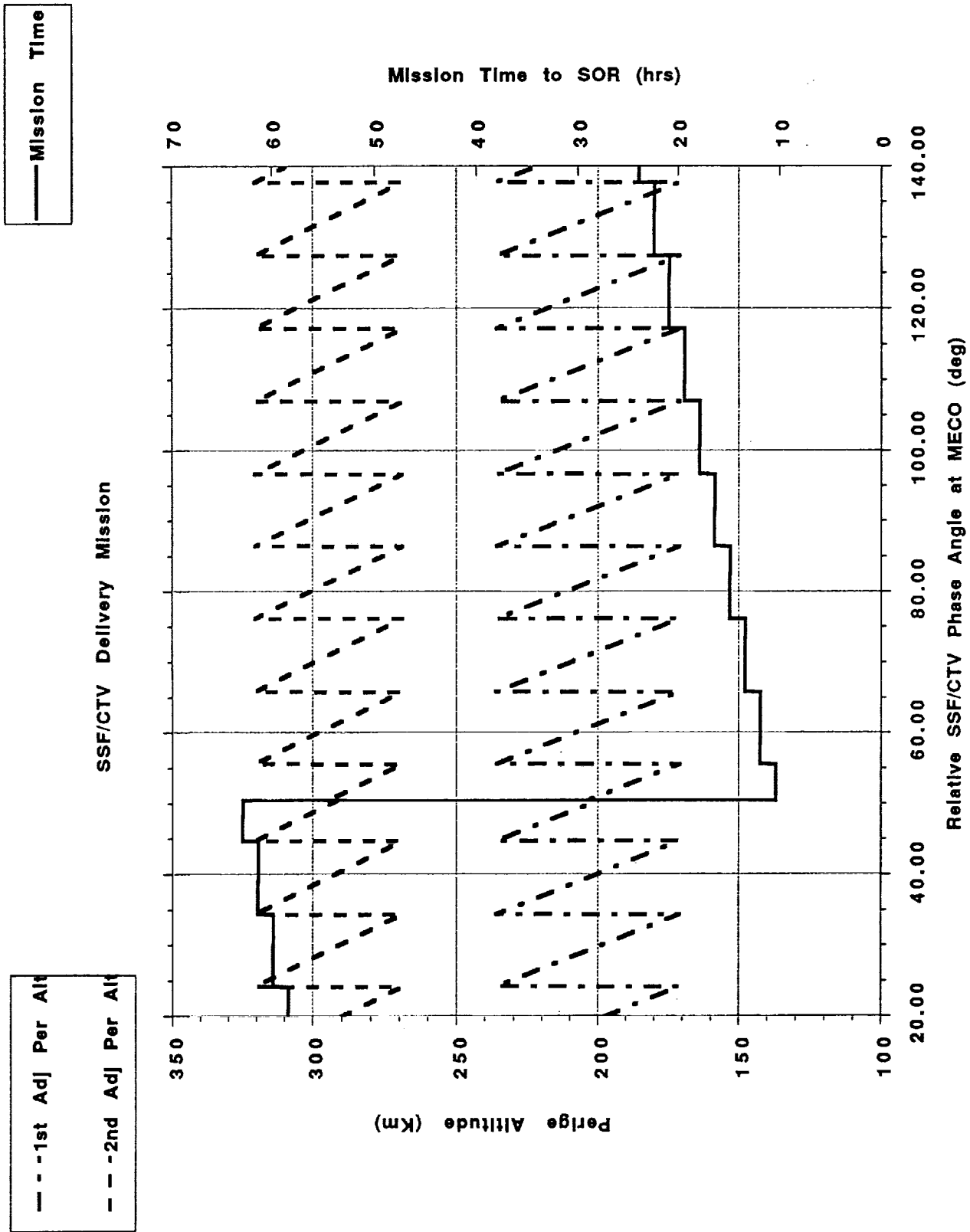Figure A3. Perigee altitude of second adjustable phasing orbit.
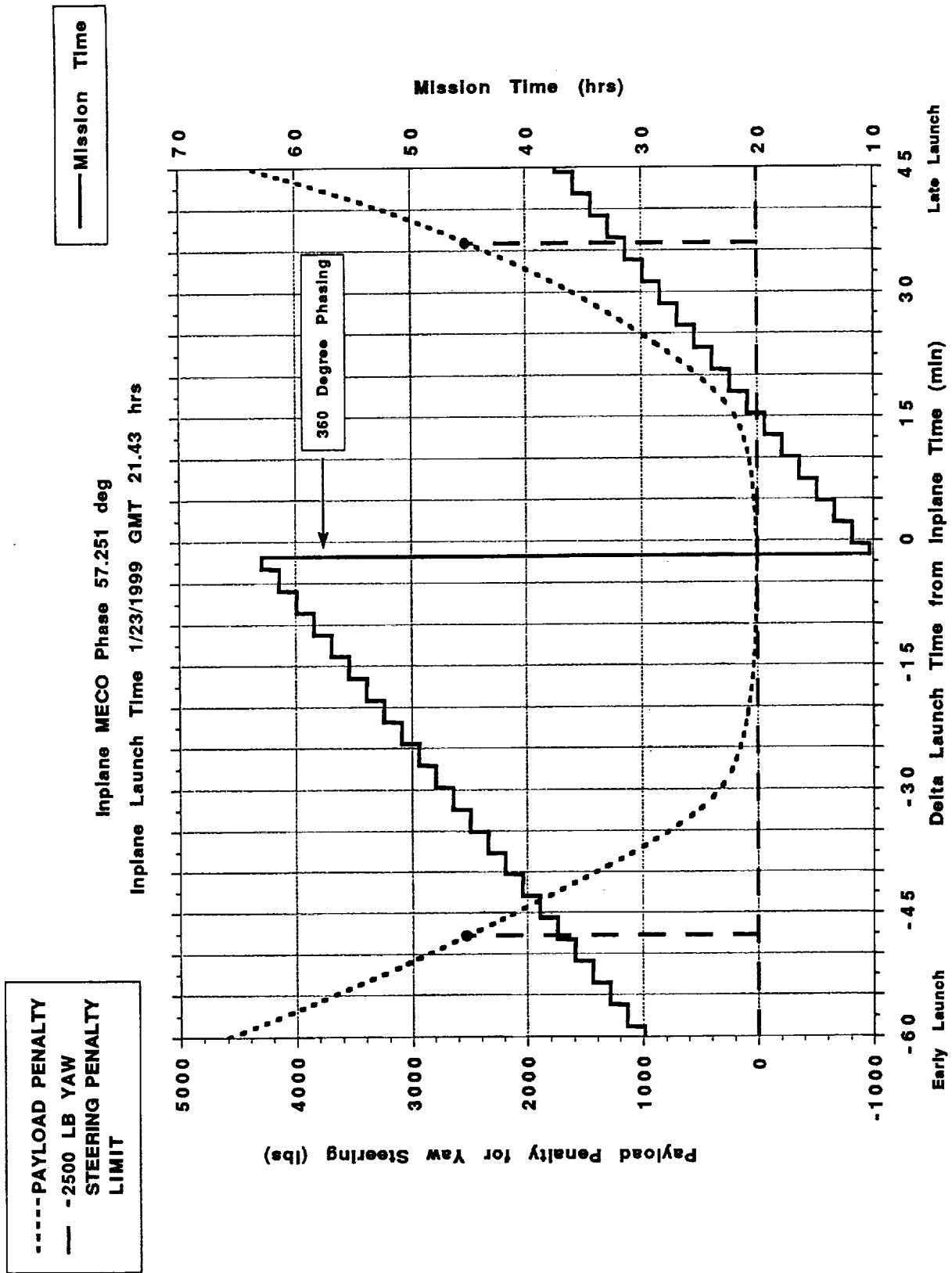
39

Figure A4. Launch window data.

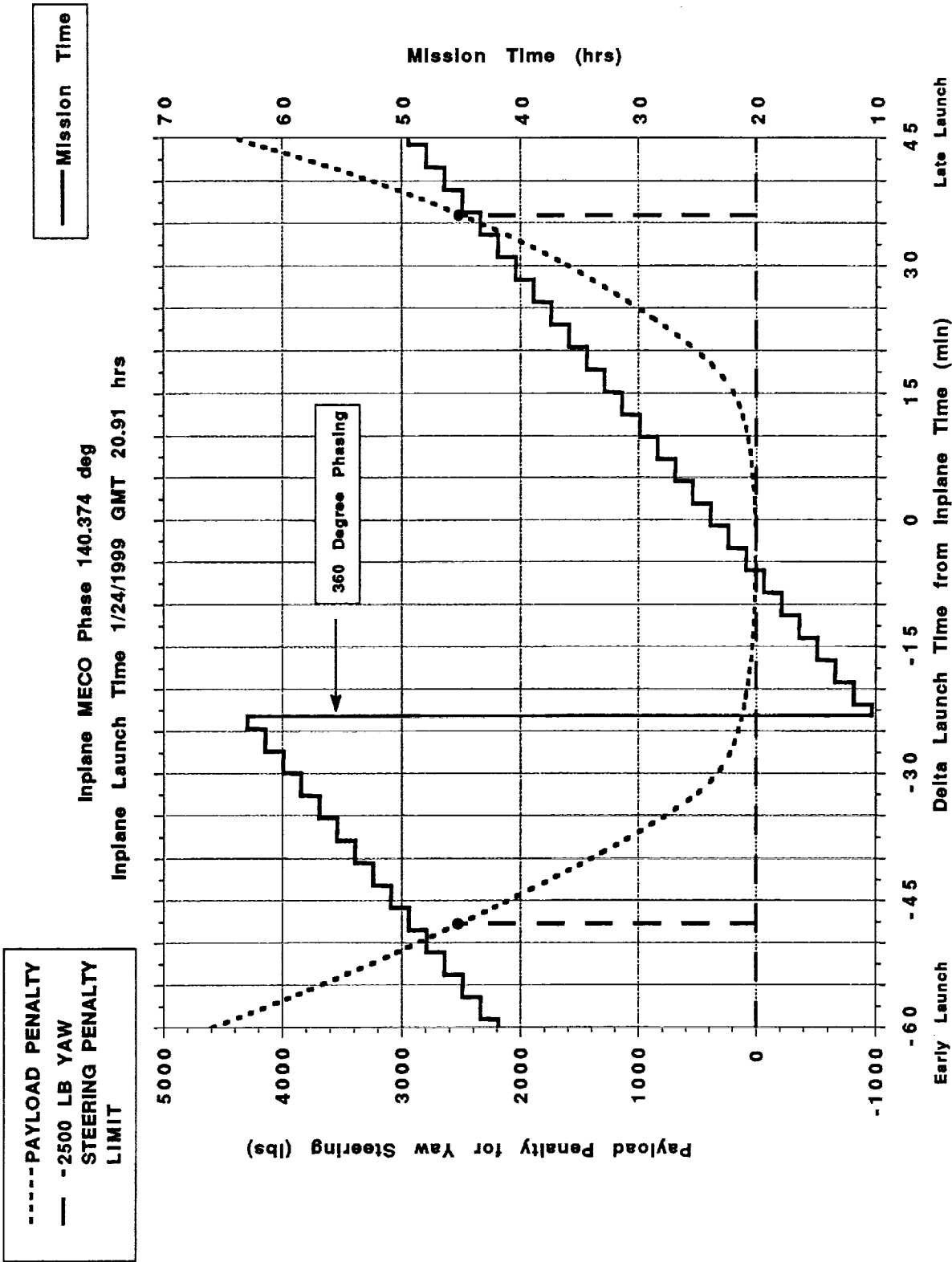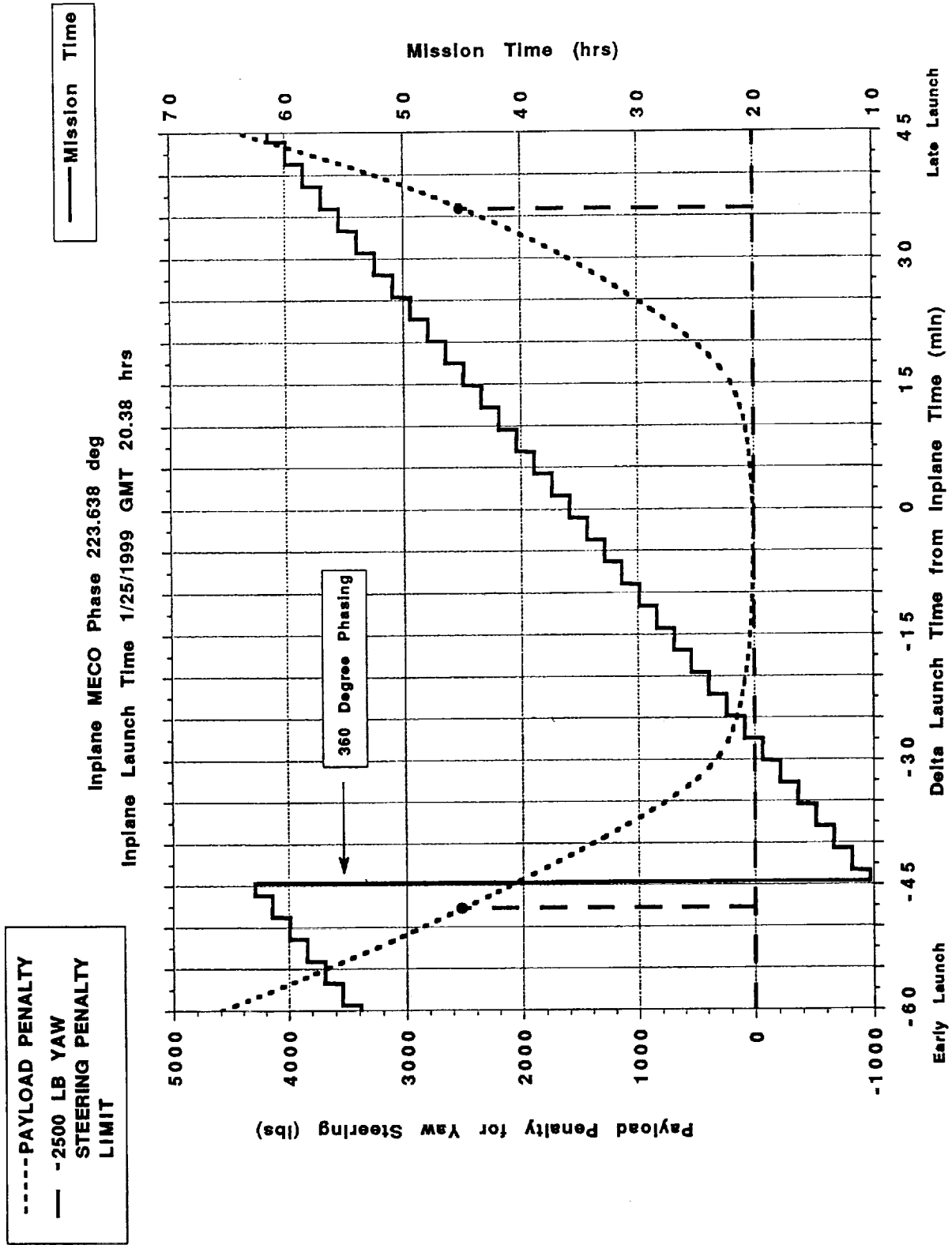Figure A5. Launch window data.

41

Figure A6. Launch window data.
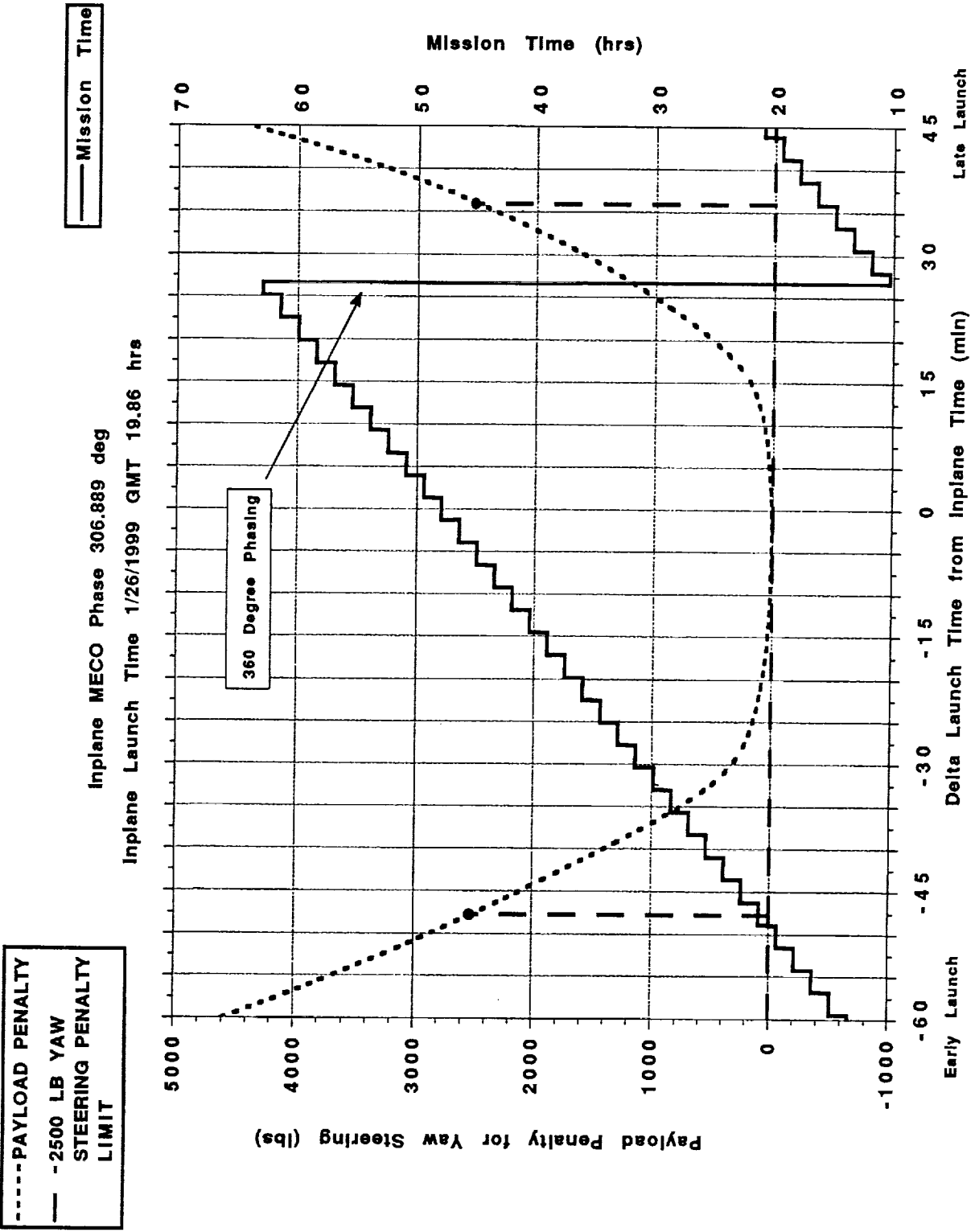
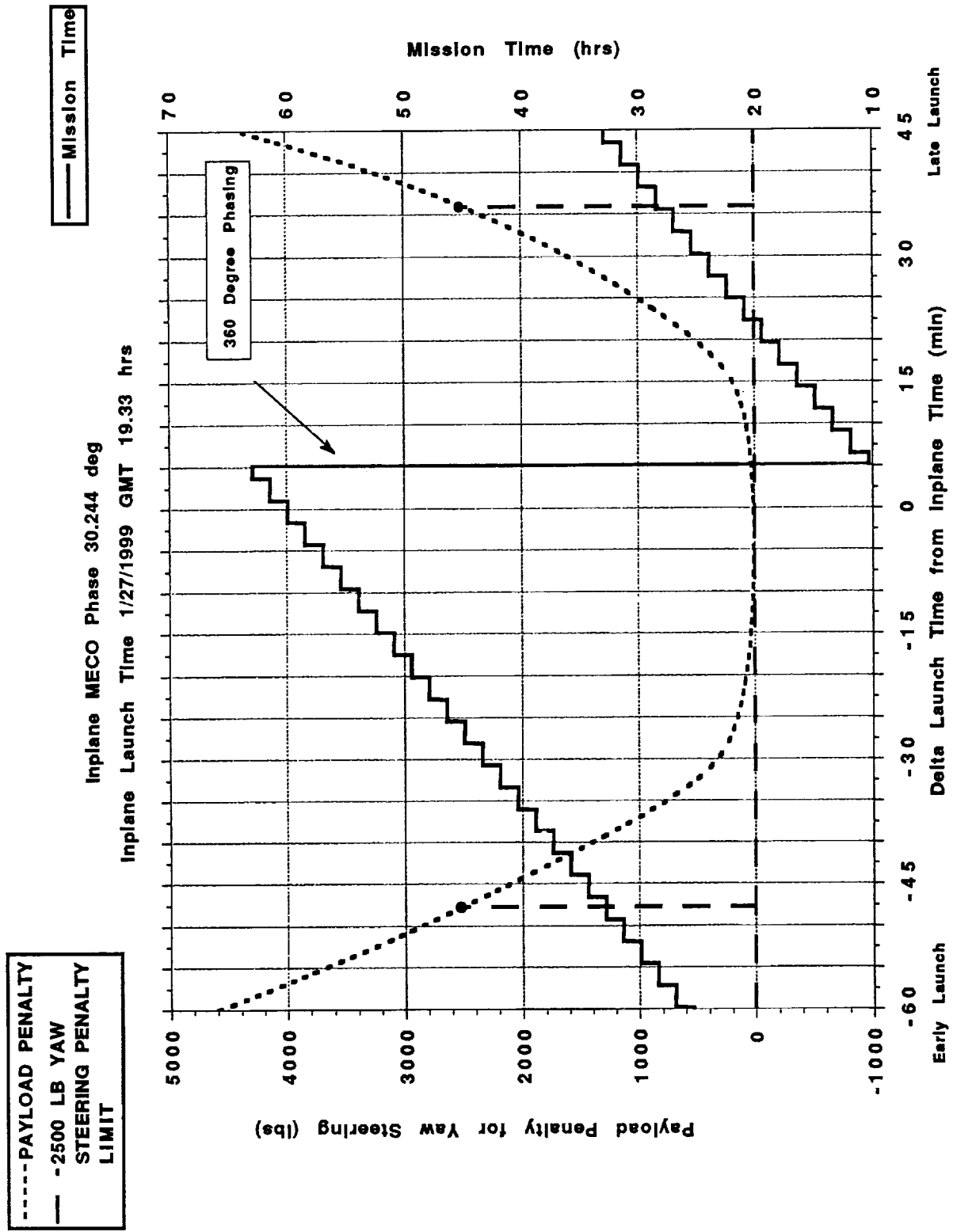Figure A7. Launch window data.

43

Figure A8. Launch window data.

44

Figure A9. Launch window data.
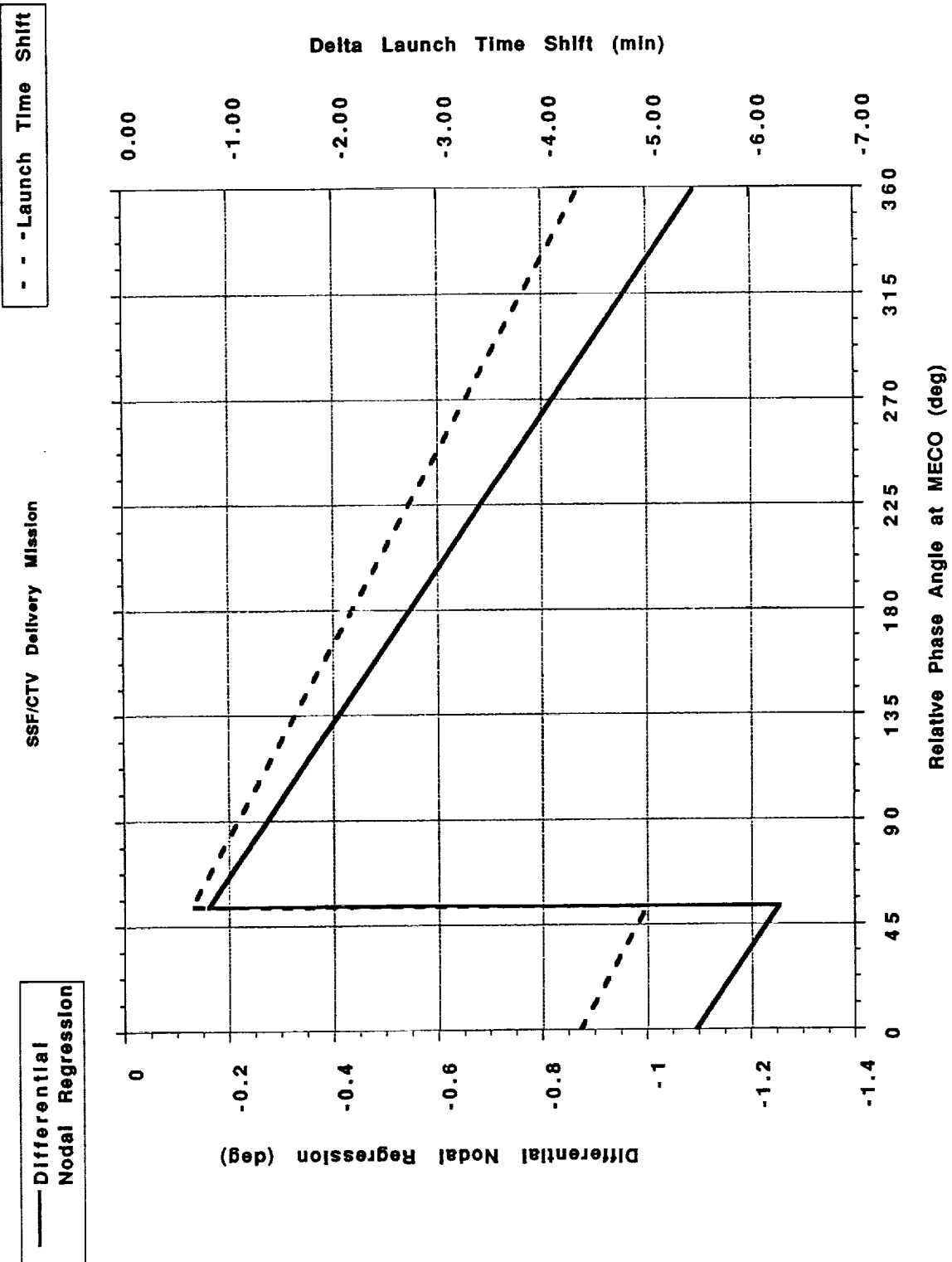
Figure A10. Launch window nodal bias correction.

APPENDIX B

Acronyms and Symbols

ACRONYMS

AN	ascending node
AP	semimajor axis of pursuit vehicle
ASRM	advanced solid rocket motors
AVG	average
AZ	azimuth (or launch azimuth)
CTV	cargo transfer vehicle
deg	degree
EOM	equations of motion
ET	external tank
GMT	Greenwich mean time
GPS	global positioning system
GST	Greenwich sidereal time
HLLV	heavy lift launch vehicle
km	kilometer
KSC	Kennedy Space Center
LT	launch time
MECO	main engine cutoff
MET	mission elapsed time
MDL	mission data load
nmi	nautical mile
POST	Program to Optimize Simulated Trajectories

PV	pursuit vehicle
RAN	right ascension of the ascending node (also represented by the Greek symbol, Ω)
RAP	radius of apogee of pursuit vehicle
RPP	radius of perigee of pursuit vehicle
RSRM	redesigned solid rocket motors
S/C	spacecraft
S/W	software
SOR	stable orbit rendezvous
SRM	solid rocket motor
S.S. *Freedom*	Space Station *Freedom*
SSME	space shuttle main engine
TBD	to be determined
TP	period of pursuit vehicle
TPI	terminal phase initiation
TT	period of target vehicle
TV	target vehicle

SYMBOLS

a	semimajor axis
e	eccentricity
i	inclination
v	true anomaly
M	mean anomaly
E	eccentric anomaly
u	argument of latitude $(= \omega + v)$

48

n	mean motion
$\bar{n}$	average mean motion
V	velocity
R	radius
γ	vernal equinox
ε	obliquity of the ecliptic plane ($\approx 23.44°$)
λ	longitude
λ_{AN}	longitude of the ascending node
ω_E	rotational rate of the Earth ($\approx 15.041°/\text{hr}$)
ω	argument of perigee
Ω	right ascension of ascending node
φ	($=\Delta u$) phase angle
ΔLT	delta launch time (measured from 0 at in-plane launch)
ΔV	delta velocity (instantaneous change in velocity)
$\Delta \varphi$	change in phase angle

APPROVAL

A PLAN FOR SPACECRAFT AUTOMATED RENDEZVOUS

By A.W. Deaton, J.J. Lomas, and L.D. Mullins

The information in this report has been reviewed for technical content. Review of any information concerning Department of Defense or nuclear energy activities or programs has been made by the MSFC Security Classification Officer. This report, in its entirety, has been determined to be unclassified.

W.B. CHUBB
Director, Systems Analysis and Integration Laboratory